

The nitrogen budget of laboratory-simulated western U.S. wildfires during the FIREX 2016 FireLab study

James M. Roberts¹, Chelsea E. Stockwell^{1,2@}, Robert J. Yokelson³, Joost de Gouw^{1,2,5}, Yong Liu⁴, Vanessa Selimovic³, Abigail R. Koss^{1,2,5*}, Kanako Sekimoto^{1,2,6}, Matthew M. Coggon^{1,2}, Bin Yuan^{1,2,†}, Kyle J. Zarzana^{1,2,Δ}, Steven S. Brown¹, Cristina Santin⁷, Stefan H. Doerr⁷, and Carsten Warneke^{1,2}

¹NOAA Earth System Research Laboratories (ESRL), Chemical Sciences Laboratory, Boulder, CO, USA.

²Cooperative Institute for Research in Environmental Sciences, University of Colorado Boulder, Boulder, CO, USA.

³Department of Chemistry and Biochemistry, University of Montana, Missoula, MT, USA.

⁴Department of Chemistry, University of Colorado, Denver, Denver, Colorado, USA.

⁵Department of Chemistry, University of Colorado Boulder, Boulder, CO, USA.

⁶Graduate School of Nanobioscience, Yokohama City University, Yokohama, Japan.

⁷Departments of Geography and Biosciences, Swansea University, Swansea, UK.

* now at Tofwerk, USA, Boulder, CO, USA.

† now at Institute for Environmental and Climate Research, Jinan University, Guangzhou, China.

@ now at Scientific Aviation, Boulder, CO., USA.

Δ now at Department of Chemistry, University of Colorado Boulder, Boulder, CO, USA.

Correspondence to: James M. Roberts (james.m.roberts@noaa.gov)

Abstract. Reactive nitrogen (N_r , defined as all nitrogen-containing compounds except for N_2 and N_2O) is one of the most important classes of compounds emitted from wildfire, as N_r impacts both atmospheric oxidation processes and particle formation chemistry. In addition, several N_r compounds can contribute to health impacts from wildfires. Understanding the impacts of wildfire on the atmosphere requires a thorough description of N_r emissions. Total reactive nitrogen was measured by catalytic conversion to NO and detection by NO-O₃ chemiluminescence together with individual N_r species during a series of laboratory fires of fuels characteristic of Western U.S. wildfires, conducted as part of the FIREX FireLab 2016 study. Data from 75 stack fires were analyzed to examine the systematics of nitrogen emissions. The measured N_r /total-carbon ratios averaged 0.37% for fuels characteristic of western North America and these gas phase emissions were compared with fuel and residue N/C ratios and mass to estimate that a mean (\pm std. dev.) of 0.68 (\pm 0.14) of fuel nitrogen was emitted as N_2 and N_2O . The N_r detected as speciated individual compounds included: nitric oxide (NO), nitrogen dioxide (NO₂), nitrous acid (HONO), isocyanic acid (HNCO), hydrogen cyanide (HCN), ammonia (NH₃), and 44 nitrogen-containing volatile organic compounds (NVOCs). The sum of these measured individual N_r compounds averaged 84.8 (\pm 9.8)% relative to the total N_r , and much of the 15.2% “unaccounted” N_r is expected to be particle-bound species, not included in this analysis.

A number of key species, e.g. HNCO, HCN and HONO, were confirmed not to correlate only with flaming or only with smoldering combustion when using modified combustion efficiency ($MCE = CO_2/(CO + CO_2)$) as a rough indicator. However, the systematic variations of the abundance of these species relative to other nitrogen-containing species were successfully modeled using positive matrix factorization (PMF). Three distinct factors were found for the emissions from combined coniferous fuels, aligning with our understanding of combustion chemistry in different temperature ranges: a combustion factor (Comb-N) (800-1200°C) with emissions of the inorganic compounds NO, NO₂ and HONO, and a minor contribution from organic nitro compounds (R-NO₂); a high-

temperature pyrolysis factor (HT-N) (500-800°C) with emissions of HNCO, HCN and nitriles; and a low-temperature pyrolysis factor (LT-N) (<500°C) with mostly ammonia, and NVOCs. The temperature ranges specified are based on known combustion and pyrolysis chemistry considerations. The mix of emissions in the PMF factors from chaparral fuels (manzanita and chamise) had a slightly different composition: the Comb-N factor was also mostly NO, with small amounts of HNCO, HONO and NH₃, the HT-N factor was dominated by NO₂ and had HONO, HCN, and HNCO, and the LT-N factor was mostly NH₃ with a slight amount of NO contributing. In both cases, the Comb-N factor correlated best with CO₂ emission, while the HT-N factors from coniferous fuels correlated closely with the high temperature VOC factors recently reported by Sekimoto et al., (2018) and the LT-N had some correspondence to the LT-VOC factors. As a consequence, CO₂ is recommended as a marker for combustion N_r emissions, HCN is recommended as a marker for HT-N emissions and the family NH₃/particle ammonium is recommended as a marker for LT-N emissions.

1 Introduction

Wildfires have severe impacts on the chemistry of the atmosphere from local to global scales (Crutzen and Andreae, 1990). A warmer, drier climate in western North America, coupled with policies that have allowed build-up of fuels in forest ecosystems has led to increases in frequency and severity of wildfires in this region (Abatzoglou and Williams, 2016; Westerling et al., 2006). The new strategy for management of wildfire in the U.S. is to allow fire where possible and to fight fire where needed (Lee et al., 2014). The science behind making these decisions and understanding their consequences involves, in part, a better understanding of the emissions from wildfires. The NOAA FIREX (Fire Influence on Regional and Global Environments Experiment) FireLab experiment was conducted in the Fall of 2016, at the U.S. Forest Service Fire Sciences Laboratory in Missoula, Montana, to acquire detailed measurements of particle and gas-phase emissions from fires involving fuels characteristic of the western U.S. (NOAA, 2018). Several aspects of these measurements dealing with VOC species, and individual reactive nitrogen species (N_r, defined as all nitrogen compounds except for N₂ and N₂O) have already been published (Koss et al., 2018; Manfred et al., 2018; Sekimoto et al., 2018; Selimovic et al., 2018; Zarzana et al., 2018), including emissions factors for many of the N_r-species (Koss et al., 2018).

The N_r compounds emitted by natural-convection biomass burning (BB) arise solely from the N in the fuels, since the combustion temperatures are not high enough (<1200°C) to produce oxides of nitrogen (NO_x) from N₂ and O₂ (the so-called Zeldovich or thermal nitrogen cycle) (Lobert and Warnatz, 1993; Taylor et al., 2004; Wotton et al., 2012). The fuel nitrogen cycles that pertain to BB flaming combustion are shown schematically in Figure 1 (Glarborg et al., 2018; Lobert and Warnatz, 1993; Lucassen et al., 2012; Manion et al., 2015). Note that the equations shown in Figure 1 are meant to indicate the general flow of the chemistry and do not always convey the mechanistic subtleties of the reactions, which are fully covered in specialized references (Glarborg et al., 2018; Manion et al., 2015). N_r compounds are emitted as small molecules, hydrogen cyanide (HCN), isocyanic acid (HNCO), and ammonia (NH₃) resulting from pyrolysis of the fuel, with minor contributions from larger N-containing organic species, especially at lower temperatures. Flame chemistry converts those species to N₂, N₂O, nitric oxide (NO), nitrogen dioxide (NO₂), and nitrous acid (HONO) as a result of radical chemistry. It has been recognized for some time that a significant

81 amount of denitrification (conversion of N_r compounds to N_2) occurs due to reactions of NO with NH_i (where $i = 1, 2,$
82 or 3) or N atoms, as confirmed experimentally (Kuhlbusch et al., 1991). While N atoms are also intermediates in the
83 thermal NO_x cycle and the reaction $N + O_2 \rightarrow NO + O$ figures in to both the fuel and thermal NO_x cycles, the second
84 reaction of the thermal NO_x cycle, $O + N_2 \rightarrow NO + N$, is too slow at BB flame temperatures to result in NO_x production
85 (Manion et al., 2015). In addition to the small molecules shown in Figure 1, numerous N_r -compounds are emitted in
86 roughly the following categories: amides, amines, heterocyclic compounds, nitriles, isocyanates, and nitro compounds
87 (Andreae, 2019; Andreae and Merlet, 2001; Koss et al., 2018; Lobert et al., 1991; Lobert et al., 1990; Lobert and
88 Warnatz, 1993; Stockwell et al., 2015). These compounds are produced at much lower abundance from fuel pyrolysis
89 and partial reactions with the radical species in Figure 1.

90 The emissions of N-compounds from BB and wildfires in general have been the subject of considerable
91 research. Early studies by Lobert et al., (1990, 1991, 1993) measured a wide range of N_r compounds in laboratory
92 fires and suggested that considerable denitrification (conversion of fuel nitrogen to N_2) was taking place, a process
93 later confirmed in experiments described by Kuhlbusch et al., (1991). Subsequent work on laboratory fires has better
94 defined particle phase nitrogen emissions (McMeeking et al., 2009) and led to the recognition of the importance of
95 several inorganic N_r species, such as HONO and HNCO (Burling et al., 2010; Roberts et al., 2011; Veres et al., 2010),
96 and the presence of a wider variety of organic N_r species (Gilman et al., 2015; Stockwell et al., 2015; Warneke et al.,
97 2011). A number of studies have sought to summarize both real world and laboratory emissions of N_r compounds
98 (Akagi et al., 2011; Andreae, 2019; Andreae and Merlet, 2001; Coggon et al., 2016; Yokelson et al., 2013b; Yokelson
99 et al., 2009). The known N-compounds range in oxidation state from NH_3 to HNO_3 and include N_2 and N_2O . Among
100 the more prominent and important N_r species are: NO_x (NO and NO_2) which is a key player in the atmospheric oxidant
101 cycle; NH_3 which has a major role in particle formation; nitrous acid (HONO) which can be an important radical
102 source; HCN and acetonitrile (CH_3CN) which are toxic at high concentrations and represent valuable tracers for
103 following fire transport; and isocyanates, HNCO and methyl isocyanate (CH_3NCO) which have unique health impacts
104 (Roberts et al., 2011). In addition, nitro ($-NO_2$), or nitrogen heterocyclic compounds may contribute to so-called brown
105 carbon, aerosol organic compounds exhibiting optical absorption in the near-UV or blue wavelength regions. Wildfire
106 N emissions also have very minor contributions from gas phase nitric acid (HNO_3). Nitric acid is either not efficiently
107 produced by BB or is readily incorporated into aerosol if it is produced in fresh wildfire plumes, as is clear from the
108 absence of HNO_3 enhancements in several studies of BB plumes (Liu et al., 2016; Yokelson et al., 2009) Alvarado et
109 al., 2010), however nitrate (NO_3^-) has been shown to contribute to aerosol mass particularly for inefficient combustion
110 (May et al., 2014). Flame chemistry is inefficient in forming N_2O , relative to the pathways that form N_2 (Andreae,
111 2019; Andreae and Merlet, 2001; Griffith et al., 1991; Hao et al., 1991). The modeling of the emissions of these N-
112 compounds on a large scale could benefit from a better understanding of the total budget of these species as a function
113 of fuel nitrogen content and the dependence of the individual species on fuel type and combustion conditions.

114 The construction of N_r -budgets in this work is made possible by the inclusion of a total reactive nitrogen
115 measurement (termed N_r herein), a method by which all nitrogen compounds besides N_2 and N_2O are converted to NO
116 and detected by $NO-O_3$ chemiluminescence. This technology has been developed by a number of groups, typically
117 using precious metal or NiCr catalysts that have been shown to convert all N_r compounds to NO (and to some extent

118 NO₂) at high temperatures (750-825°C) (Hardy and Knarr, 1982; Kashihiro et al., 1982; Marx et al., 2012; Roberts et
119 al., 1988). There are also commercial instruments that incorporate this technology (see for example Thermo Scientific
120 Model 17i). This technique has been applied to gas phase atmospheric measurements, principally to measure NH₃ by
121 difference techniques (Saylor et al., 2010; Schwab et al., 2007), and has also been used to observe wildfire plumes
122 that have impacted ambient air measurements (Benedict et al., 2017; Prenni et al., 2014). We have recently developed
123 a platinum/molybdenum oxide N_r catalyst system, and confirmed that it quantitatively converts N_r compounds
124 including all particle-bound nitrogen compounds (Stockwell et al., 2018). To our knowledge this technique has not
125 been applied directly to BB emissions before.

126 This paper ~~will~~ describes the total reactive nitrogen, and individual N_r compound measurements made during
127 the FireLab 2016 experiment, with the intent of providing information that can be used for analysis and modeling of
128 the impact of wildfire emissions on the atmosphere. The total N_r measurements ~~will be~~ are combined with CO₂, CO,
129 and VOC measurements and fuel, residue and ash C and N content to estimate the amount of N lost to N₂ and N₂O. In
130 addition systematics of the ratio N_r/Total Carbon are examined for simplifying relationships. Fire-integrated N_r ~~will~~
131 ~~be~~ is then compared to fire-integrated measurements of individual compounds to determine the fraction of
132 unaccounted-for N_r. The systematic behavior of individual N_r species and their fractional contribution to N_r ~~will be~~
133 ~~are~~ examined with respect to fuel type, N content, and combustion processes. A positive matrix factorization (PMF)
134 technique ~~will be~~ is used to examine commonalities between fires of different fuels under different conditions and
135 compared to the PMF analysis of the VOC emissions published by Sekimoto et al., (2018). The results ~~will be~~ are
136 used to arrive at suggested guidelines that can be used estimate N_r-emissions profiles for fires representative of western
137 North America.

138 139 2 Methodology

140 The FireLab 2016 study involved laboratory burns of fuels mostly characteristic of western North American
141 wildfires such as coniferous fuels and chaparral fuels (important in central to southern California and the southwestern
142 U.S.). We also measured some that have global significance such as Indonesian peat and yak dung (important in areas
143 above timberline or where wood is scarce, such as India, Nepal, and Tibet). The procedures and associated details of
144 the study have been described previously by Selimovic et al., (2018) and will be only briefly summarized here. The
145 detailed data on fuel types, amounts and composition can be found in Table S1, and in the Supplemental section of
146 Selimovic, et al., (2018). The laboratory burns involved fuel samples, ranging in mass from 0.26 to 6.02 kg spread out
147 on a fuel bed roughly 1m x 1m square. Fires were started without the addition of any contaminants, using an electric
148 igniter (a series of NiCr heating elements that were flash-heated electrically), and typically lasted from approximately
149 5 to 30 minutes. Seventy-five fires were conducted in the “stack” burn configuration where the smoke was directed
150 up the central stack of the facility where it could be sampled simultaneously by all the instruments that measured gas
151 phase species, and some of the particle phase measurements. The sampling platform was about 15 m above the fire
152 and the sampling took place in well-mixed smoke approximately 5s after emission (Christian et al., 2004). Thirty-one
153 additional fires were conducted as “room” burns on most of the same fuels, when the stack was closed and the room
154 was allowed to fill with smoke, permitting sampling to be done over the course of several hours. The following

analyses will focus on the “stack” burns, as those measurements had little or no interferences from surfaces, where “room” burns are known to be compromised by the loss of materials, such as NH_3 , to the room walls at long sample times (Stockwell et al., 2014). Ash analyses were performed only on the residues from the room burns and those values will be used for the N and C budget calculations, with the assumption that stack and room burns left similar ash considering the combustion conditions were the same for each type of fire. Table 1 lists the compounds and associated techniques used to measure them during the FireLab 2016 study, and describes the grouping of NVOCs measured by PTR-ToF into common categories, e.g. amines, nitriles, etc. We specifically note that the OP-FTIR is capable of measuring gas phase HNO_3 with comparatively good sensitivity (10ppbv detection limit in fires where N_r can be 5 ppmv or more), but HNO_3 was not observed above detection limit in any of the fires.

2.1 N_r and NO measurements by Chemiluminescence

Total reactive N (N_r) was measured by catalytic conversion to NO, followed by O_3 -chemiluminescence using an instrument described previously (Williams et al., 1998). N_r and NO were sampled from inlets inserted adjacent to the inlet-less open-path Fourier transform infrared spectrometer (OP-FTIR) instrument path during the stack burns (Selimovic et al., 2018), and from a platform approximately 4 m off the floor in the middle of the room during the room burns. The catalyst used for the N_r channel, described in detail by Stockwell et al. (2018), consisted of a 11 mm I.D. quartz tube, packed with 36 platinum screens, heated to 750°C. This tube was wrapped with high temperature heating tape and insulated inside a 7cm OD stainless steel tube that was fitted to a bulkhead placed through the wall of the stack. The N_r channel was diluted by a factor of 5:1 ($\pm 3\%$) using a flow of zero air added immediately downstream of the Pt catalyst assembly. NO was sampled through a 6.3mm O.D. stainless steel inlet tube which was placed through the bulkhead directly into the free air stream of the stack and connected to a 50mm Teflon filter holder immediately outside the stack. The transfer lines for the N_r and NO measurements consisted of 6.35mm O.D, 1mm wall thickness PFA tubing of approximately 20 m in length. N_r and NO data were acquired at 1 s frequency, but the flow rate through each inlet was 1 SL min^{-1} , resulting in residence time in each inlet of 14 s. This time delay was corrected in the data analysis. Any chemical effects of the inlet on the sampled air stream were negligible since the analytes consisted of only NO and NO_2 and those are known to be transmitted by PFA Teflon tubing with essentially no surface effects. However, there were possible effects of the inlets on the temporal features of the measurement through diffusion or turbulent mixing. Those effects were examined through comparison of the temporal variations in the NO signal with the NO measured by the OP-FTIR, and comparison of the N_r signal under smoldering conditions with the NH_3 measured by the OP-FTIR. Both of these comparisons showed that the NO and N_r inlets had effective time constants of 4 seconds, somewhat slower than the diffusive relaxation time assuming solely laminar flow. Examples of the estimate of diffusion and dispersion on NO and N_r signals, and the estimate of the effective time constant of these measurements are presented in the Supplemental Information.

The inlet streams were sampled by the NO instrument either directly (NO channel) or after passing through a second catalyst of molybdenum oxide (MoO_x) to convert remaining NO_2 to NO. The MoO_x catalyst consisted of a molybdenum tube at 350°C to which a small flow of H_2 (0.8%v/v) was added to control the re-dox state of the surface. Both channels of the instrument were “de-tuned” to keep raw photon count rates below 4 MHz, by turning down the

O₃ flows and PMT voltages. Calibrations were performed with both a NO standard in N₂ (Scott-Marrin) and 10.1 ppmv standard of HCN in nitrogen (Gasco). The Pt catalyst was dismounted from the stack (or room) every few days and checked for conversion efficiency by the addition of the HCN standard to the inlet. Conversion efficiencies were found to be consistently high (>98%) throughout the entire sampling period (October 5 – November 12, 2016). There were slight background signals (a few tens of ppbv) for both NO and N_r in both the stack and room air prior to and after the burns, and those were subtracted from the fires signals prior to reporting the data. The overall uncertainties in the NO and N_r data were ±10% for each measurement.

2.2 Other measurements

Measurements of individual species during the 2016 FireLab study have been presented in several previous publications. The OP-FTIR measurements were discussed by Selimovic et al., 2018, and the PTR-ToF measurements were discussed by Koss et al., (2018). In addition, some of the calibration methods and GC separation and identifications rely on additional analytical work presented by Sekimoto et al., (2017) and Gilman et al., (2015). We measured the mass and elemental content of the initial fuel and the mass of unburned fuel for all the fires, and we measured the mass and the elemental content of the ash during 21 room burns, which covered all the fuel types discussed.

2.3 PMF Analysis

Trace gas measurements from multiple instruments involved in the FireLab study were combined and analyzed using positive matrix factorization (PMF). PMF is a numerical method that was used in this case to partition the compounds involved in a time varying mixture of chemicals into a few groups, or “factors”, where a compound can appear in more than one factor. A factor represents a consistent profile of compounds that is representative of one of the sources contributing to the total signal. The sum of all the “factors” then ideally describes the total composition of the measurements, which in this case is the emissions of N_r compounds. By its nature, PMF assumes that the total signal is a linear combination of individual sources that have a consistent composition, the relative contribution of which is represented by the amount of each compound or category found in each factor (Paatero and Tapper, 1994; Ulbrich et al., 2009). We hypothesize that species with dominant fractions in the same factor are related to each other via the same formation processes. With knowledge of factor composition and the amount of each factor at any given time the original emissions measurements can be reconstructed and this approach provides an alternate source of profiles for fire emissions. PMF has also been used by a number of groups to explore how much various source profiles contribute to complex ambient measurements (see for example Ulbrich et al., 2009) and was recently used to analyze PTR-ToF-MS measurements from the FireLab (Sekimoto et al., 2018). Here, PMF was accomplished using the PMF Evaluation Tool v. 2.08A (Ulbrich et al., 2009).

The application of PMF to this data set is different than the instances where it is applied to data from a single instrument in which compound abundances are inherently scaled properly and error estimates are well defined and self-consistent. For example, when applied to mass spectral data from a single instrument, errors can be expected to scale as the square root of ion counts based on fundamental counting statistics (Sekimoto et al., 2018). In this work

we are including nitrogen measurements from several instruments, thus we chose to use mixing ratios as the unit of comparison. The error estimates required by the PMF analysis were taken from the reported combined uncertainties: the sum of the detection limit plus the estimated random error of the measured value. For example, the uncertainty in a NO mixing ratio of 500ppbv was ± 51 ppbv. The variables that were used in this PMF analysis and their units and corresponding errors are listed in Table 2. Where compound categories are specified (e.g. nitriles), the values were the sum of the measured compounds in that category as listed in the footnotes to Table 1. The data were further adjusted by subtracting the ambient air background before and after the fires, which was a relatively minor adjustment for most compounds and categories. Any negative numbers that resulted were very small compared to the fire emissions, and were set to zero. In addition to the PMF analysis for the species listed in Table 2, several exploratory runs were tried with CO₂, CO added (in units of ppmv) and total N_r (in units of ppbv) added to the list in Table 2. No significant differences were observed in the results for individual N_r compounds and classes, so CO₂, CO and Total N_r were not included in this analysis.

Two approaches were taken when performing PMF analyses. The first approach included all individual N-containing compounds together with CO₂, CO, and N_r in the analysis batch (Batch 1), while the second excluded the latter three species (Batch 2). CO₂ and CO were included because of their well known roles as indicators of flaming and smoldering combustion, respectively, an effect traditionally captured through the use of Modified Combustion Efficiency (MCE) defined as

$$MCE = ACO_2 / (ACO_2 + ACO) \quad (Eq. 1)$$

where ACO₂ and ACO are the CO₂ and CO levels above the ambient. When CO₂ and CO were included, the carbon species were put into the PMF in units of ppmv, and all the nitrogen species in units of ppbv. This was done because the nitrogen levels were on the order of a percent or less compared to the carbon species. The second analysis batch (Batch 2) involved only the individually measured nitrogen species and categories listed in Table 1 so that factor loadings would be reflective of the nitrogen-only emissions. Batch 2 factors indicate how N_r species are related to each other via combustion chemistry.

We applied PMF to single fire data as well as extended time series that included all fires of a particular fuel type, in-line with the approach laid out by Sekimoto et al., 2018. By consolidating fuels from a particular vegetation type, the fire to fire variability largely driven by differences in the fuel (e.g. moisture content, structure, quantity) is constrained and the most representative fire conditions are captured. Two fuel groups were analyzed in this way: the western U.S. coniferous ecosystem fuels which included ponderosa pine, lodgepole pine, Douglas fir, Engelmann spruce, and sub-alpine fir and the Southwestern U.S. chaparral ecosystem which was represented by chamise and manzanita. The consolidated time series for the coniferous ecosystems included realistic mixtures, canopy only, and litter only, while duff and rotten logs were analyzed separately, and not included in the timeseries.

3 Results and Discussion

The measurements of total N_r can be combined with N and C measurements of fuel and ash to estimate N lost to N_2 and N_2O . The total N_r emitted from laboratory fires combined with individual N compound measurements allow us to construct a budget for N_r species that define what the dominant forms of N are and how those emissions depend on other fire parameters, or different temperature combustion processes. The systematics of N emissions found by PMF are compared to other fire indicators and PMF analyses previously conducted on VOCs allow the formulation of simplifying relationships that can be used in atmospheric models of wildfires.

3.1 Comparison of N_r and Total Carbon in fire emissions

The total N_r and total carbon emissions were measured for 75 stack fires in order to place the N emissions in the context of total carbon which has been widely estimated for wildfires. Example timeseries of NO , N_r , ΔCO , ΔCO_2 (CO and CO_2 corrected for their backgrounds) are shown in Figure 2, for a fire burning a sample of ponderosa pine realistic mix (Fire 004). In addition to the chemical species, the modified combustion efficiency (MCE) was also plotted. MCE is defined as

$$MCE = \Delta CO_2 / (\Delta CO_2 + \Delta CO) \quad (Eq. 1)$$

where ΔCO_2 and ΔCO are the CO_2 and CO levels above the ambient. MCE has traditionally been used to indicate the relative amount of flaming and smoldering combustion in a fire. The timeseries for Fire 004 (Figure 2) shows a short initial smoldering/distillation phase (MCE 0.7 to 0.8) as heat pyrolyzes the fresh fuel and releases VOCs from existing pools in the fuel followed after ignition by a relatively efficient mix of flaming and smoldering combustion (MCE 0.95 to 0.98) and then finally a subsequent period of essentially pure smoldering (MCE ~0.80). The N_r and NO timelines had many features in common because NO is often the most abundant N_r compound (see below). As a result, it is useful to compare the quantities N_r-NO and $(N_r-NO)/N_r$ to the other measures of chemical species or combustion efficiency. As expected, $(N_r-NO)/N_r$ in Figure 2(c) is anti-correlated with MCE since N_r is primarily NO at high MCE. In addition to the anti-correlation, this non- NO fraction, like its approximate carbon analog CO/CO_2 , has a wider dynamic range than MCE and will often suffer less from background variability than carbon-based indices (Yokelson et al., 2013a).

The concentration profiles of the background-corrected measurements of N_r , CO_2 , CO , and all the carbon-containing species measured by the FTIR (Selimovic et al., 2018) during the stack burns were integrated over the entire time of the burn to obtain total carbon, termed TC here, and total N_r . The additional carbon species included methane and a number of other gas phase VOCs as well as organic- and black-carbon aerosol. Altogether these carbon species should account for $\geq 98\%$ of emitted carbon (McMeeking et al., 2009). Total N_r is plotted in Figure 3, versus TC (Figure 3a) and versus nitrogen burned, which is calculated from the %N in the fuel \times the mass of fuel consumed (Figure 3b). The points in Figure 3 are colored by the fuel N/C mole % obtained from the elemental analysis of each fuel. The relationship between N_r and TC in panel 3a clusters around the 0.37% line and those points are from fuels most characteristic of the North American biomes impacted by wildfire. There are clear outliers in the correlation of N_r and TC; for example, yak dung and two samples of duff (Engelmann spruce and subalpine fir) were high due either

to the fact that they have high fuel N/C ratios ([dung, see Table S1](#)), or they burned with minimal flaming (whole fire MCEs 0.86-0.89, [duff and dung](#)), hence experienced less de-nitrification. The fuels that were low in N_r/TC in panel 3a, ponderosa pine rotten log, subalpine fir and excelsior, had low fuel N/C, so when plotted versus nitrogen burned in panel 3b, they cluster with the main group of characteristic fuels, i.e. they are no longer ‘outliers’ in the distribution.

[3.2 Estimates of denitrification](#)

[The removal of N to forms in-active in the troposphere, \$N_2\$ and \$N_2O\$, has importance in the biogeochemistry of forest ecosystems and also determines how much N takes part in wildfire plume chemistry.](#) The points in Figure 3a are all lower than the corresponding fuel N/C mole ratio, due to the denitrification chemistry, shown in Figure 1, and verified in lab studies described by Kuhlbusch et al. (1991), and the production of N_2O which is also not measured by the N_r technique. The sum of N_2 and N_2O produced in the fires can be estimated from the difference between the fuel N/C and the $N_r/Total\ C$ emitted and the data on C and N content remaining in the ash. The mass balance equations used for these calculations are detailed in the Supplemental Materials.

The distribution of the N lost to N_2 and N_2O is shown in Figure 4. Chemical analyses were not done for all fuels during the stack burns, and the analysis above assumes that the ash residues and ash/burned fuel ratios from the stack burns were well represented by those for the same fuels used in the room burns, for which mass yields and chemical analyses were done. Data are missing for fuels that did not have a corresponding [residue](#) analysis. The median fraction of N lost to N_2 and N_2O for ash-corrected fires was 0.70, and the mean (\pm standard deviation) was 0.68 (\pm 0.14). This fuel-based estimate is uncertain by approximately 25% because of the above assumptions concerning the applicability of the [residue](#) analyses from the room burns and because fuel moisture corrections were assumed to apply to all of the materials burned, foliage vs. woody biomass (see SI for details). The emission of N_2O relative to N_2 is approximately 10% or less for a wide range of fuels (Andreae, 2019). Assuming the N remainder in our work is at least 90% N_2 gives values that are somewhat higher than the N_2 values reported by Kuhlbusch et al., (1991) where N_2 accounted for 36% of fuel N burned in flaming stage fires. A closer inspection of Kuhlbusch et al., (1991) showed a range of N_2 yields of 40-54% at highest MCEs of 0.94-0.97. Possible reasons for these differences are that the Kuhlbusch et al., (1991) fires were limited to grasses, hay, and pine needles, and the fires were confined to a closed container and so may not have experienced the convection and turbulence of typical biomass fires. In addition, the fires analyzed in our work were somewhat weighted towards the full canopy and higher temperature burning fuels, since ash analyses were not done for peat, dung and many of the “litter” samples, all of which tend to burn less efficiently. Goode et al., (1999) estimated an N_2 emission of $45\pm5\%$ for MCE values of 0.95 in grass and surface fuels. The range of values determined in our work overlap with these literature values, but are on average higher. It should be noted that such loss of reactive nitrogen can have implications for ecosystem N budgets, as discussed by Kuhlbusch et al., (1991).

[3.3 The budget of \$N_r\$ and individual N containing species](#)

The composition of the N that does not get converted to N_2 or N_2O is of intense importance in determining atmospheric impacts of fires, [since those compounds are involved in oxidation capacity \(\$NO_x\$ \), radical production \(\$HONO\$ \) and particle formation \(\$NH_3\$ \).](#) Emission factors for all the individual N_r compounds identified in our work

339 have been compiled and reported in previous publications (Koss et al., 2018; Selimovic et al., 2018), so this paper will
 340 focus on the N_r budget. The balance of N_r budget for Fire 047, sub-alpine fir realistic mix, is shown in Figure 5, in
 341 which the timelines of N_r , NO, N_r -NO, sumN, and NVOC are plotted along with MCE and $(N_r\text{-NO})/N_r$. The quantity
 342 sumN is the sum of all other non-NO compounds, and NVOC is the subset of sumN that are organic nitrogen
 343 compounds measured by the PTR-ToF, as listed in Table 1. This fire had a mixture of flaming and smoldering
 344 combustion throughout the fire as indicated by MCE and nitrogen profiles (panel (d)). The comparison of N_r -NO with
 345 the sumN in panel (b) shows that much of the N is accounted for. The major contributors to sumN for this fire were
 346 HNCO, HCN, HONO, NO_2 , and NH_3 , while NVOC was a very small contributor to sumN (panel (b)). Note that while
 347 HNO_3 is measurable by FTIR with good sensitivity, no HNO_3 signals were observed above detection limit, which was
 348 10 ppbv. Panel (c) shows the residual left after NO and sumN are subtracted from N_r , corresponding to an integrated
 349 amount of $15.6 \pm 8\%$ of N_r . This residual is reasonable considering typical published particle N_r measurements (Akagi
 350 et al., 2012; Akagi et al., 2011; Liu et al., 2017; May et al., 2014), and consistent with there being some particle N_r
 351 from flaming, which are most likely organic nitrates or nitro-organics, and particle ammonium from smoldering with
 352 potassium or ammonium nitrate potentially accounting for substantial N_r .

353 Several fuels had much lower NO emissions and higher unaccounted for N_r . Yak dung was one such fuel the
 354 emissions of which stand in contrast to the fire shown above. The nitrogen emissions from Fire 050, yak dung, are
 355 shown in Figure S2. This fuel produced mostly smoldering emissions as exemplified by the low NO levels relative to
 356 N_r (panel a), and the low MCEs observed (panel d). The sum of N_r species was somewhat correlated with the quantity
 357 N_r -NO, but was substantially lower, and the residual N_r unaccounted for by the gas-phase measurements was 33.9
 358 $\pm 16\%$ of N_r (panel c). The majority of sumN was represented by HCN and NH_3 , with acetonitrile (CH_3CN) higher
 359 than any of the other inorganics, HNCO, NO_2 or HONO. The NVOCs were also a larger fraction of N_r -NO than in the
 360 case of Fire 047 shown above, a feature that implies that more semi-volatile organic compounds, SVOC, survive these
 361 types of fires and could make a proportionally higher contribution to the N_r budget in this fire relative to Fire 047.
 362 FireLab results of particle organic carbon measurements (Jen et al., 2019) and field measurements in environments
 363 with a lot of dung burning (Jayarathne et al., 2018; Stockwell et al., 2016a) are consistent with a higher EF for particle
 364 organic carbon and by extension particle NVOC compounds. The quantity $(N_r\text{-NO})/N_r$ was relatively high and had
 365 less dynamic range than for fires with more flaming combustion like Fire 047.

366 An overall budget of N_r can be constructed for all of the stack fires through integrating the time profile of all
 367 the compounds and compound classes. The fire-integrated measurements of inorganic and NVOC species are listed
 368 in the Supplemental section as ratios to N_r for each stack fire (Table S1). The summary of all the fire integrated X_i/N_r
 369 fractions (where X_i is the N_r species or quantity) is given in Table 3 for all the fires for which we have a complete set
 370 of measurements (43 fires). In general, NO was the major species followed by NH_3 , and the other inorganic N_r species,
 371 NO_2 , HNCO, HONO, and HCN had individual contributions of 4.3 to 9.4 %. NVOC species were less than 5% of N_r
 372 on average. The unaccounted-for N_r , defined as $(N_r\text{-NO-sumN})/N_r$ had a median value of 14.3% and a mean (\pm std.
 373 dev.) of $15 (\pm 10)\%$. Overall, 85% of N_r was accounted for by the gas phase measurements. The distribution of whole
 374 fire N_r residuals is plotted as a histogram in Figure 6. We expect the residual N_r was composed of either semi- or low-
 375 volatility compounds, or particle-bound N_r compounds, which we know are converted efficiently by the N_r catalyst

(Stockwell et al., 2018) but not detected by the instruments included in this analysis. Along these lines, there is some indication that the residual has a systematic variation with whole fire MCE, with higher residuals (up to 30%) observed at lower MCEs and higher $(N_r - NO)/N_r$ (see Figure S1 a&b), which would be consistent with higher EF for SVOC at low MCE (Jen et al., 2019) and particle N_r having a higher contribution from NO_3^- (May et al., 2014), and perhaps particle ammonium or reduced- N_r compounds. In general, there is more particulate organic material emitted from fires at low MCE (Jen et al., 2019), so we would expect more particle N at low MCE to go along with that.

3.4 Systematic dependences of N_r composition on combustion processes.

The features noted in fires shown above, as well as the anti-correlation of MCE and $(N_r - NO)/N_r$ lead to the question of whether there are systematic dependences in N_r -compound composition on fire stage that can be used to formally classify and/or potentially predict the relative emissions of N_r compounds. MCE has been used as a rough indicator of the relative amounts of flaming and smoldering combustion in a fire, with high MCE (~99%) being “pure” flaming, low MCE (~80%) being “pure smoldering,” and an MCE of ~0.9 being roughly equal amounts of both (Sect. 2.1.1 in Akagi et al., 2011). It should be understood that “smoldering” in this framework is a lumped term that includes all non-flame processes such as pyrolysis, glowing, and distillation, **which are** the processes **that produce** gaseous fuel to support **flaming** (Yokelson et al., 1996). In addition, “pure flaming” is essentially the efficient oxidation of smoldering products before they enter the atmosphere. However, for MCE to predict flaming and smoldering N_r species well, the variable fuel N must be considered. For instance, NO_x is clearly produced by flaming based on its temporal profile, but fire-integrated EF_{NO_x} may not correlate with MCE due to variable fuel N. In these cases, $EF_{NO_x}/\text{fuel N}$ or $\Delta NH_3/\Delta NO_x$ may still correlate (or anti-correlate) well with MCE (e.g. Fig. 4 in Burling et al., 2010 or Yokelson et al., 1996). Finally, the flame chemistry involving NH_3 , $HNCO$, and HCN both produces and destroys NO in a fashion that does not conserve N_r . This chemistry is explored in Figure 7 in which NO_x , NH_3 , $HNCO$, HCN , $HONO$, and CH_3CN ratios to N_r are plotted vs real-time MCE for Fire 047 as a typical example for fires that have a substantial range of MCEs (e.g. from 0.8 to above 0.98). The relationship between NH_3/N_r and MCE confirms that NH_3 is primarily a smoldering emission and NO_x/N_r increases with increasing MCE in a non-linear fashion that confirms it is primarily a flaming compound. Such a non-linear dependence has also been seen for other flaming-related quantities such as Elemental Carbon/TC or EF_{HCl} (Christian et al 2003; Stockwell et al., 2014). Most importantly, the variations of $HNCO/N_r$, HCN/N_r , $HONO/N_r$, and CH_3CN/N_r versus MCE **do not** arise dominantly from either regime as these are species that are likely produced by multiple pathways (e.g. “incomplete flaming”, pyrolysis, possibly glowing). By “incomplete” flame chemistry we mean the production of incompletely oxidized products in flames such as the complex system of reactions shown in Fig. 1. These reactions involving $HNCO$, HCN and NH_3 both produce and destroy NO , while $HONO$ is produced from reactions of NO and NO_2 that are faster at slightly lower temperatures, for example the three-body association reaction of NO with OH radical (Manion et al., 2015). Variable turbulence in the turbulent diffusion flames that are characteristic of open BB likely contributes to varying temperatures, and therefore, varying amounts of incomplete oxidation of the fuel N (Shaddix et al., 1994).

3.5 The PMF analysis of coniferous fuels

413 The complexity of the dependence of N_r speciation on combustion chemistry suggests that MCE is an
 414 insufficient model to use for applying lab results to real-world fire emissions (Stockwell et al., 2016a; Yokelson et al.,
 415 2013b). Accordingly, we employed the positive matrix factorization (PMF) method (see Methodology section) that
 416 has been used by a number of groups to probe the sources contributing to complex mixtures (see for example Ulbrich
 417 et al., 2009 Sekimoto et al., 2018). Our PMF results showed several general features, irrespective of the inclusion or
 418 exclusion of CO_2 , CO and N_r . The emissions were best fit by three factors (with approximate descriptive names
 419 justified below and prime species): (1) a combustion (flaming) factor (abbreviated Comb-N), (2) a high temperature
 420 pyrolysis factor (HT-N), and (3) a low temperature pyrolysis factor, (LT-N). We use these terms in part to harmonize
 421 our discussion with the VOC results discussed by Sekimoto 2018. An example timeseries for the PMF analysis of a
 422 coniferous fuel with just the N_r species included is shown in Figure 8 for a realistic mix of lodgepole pine (Fire 063).
 423 In this case, several different Fpeak values were tried (-1, 0, +1) and runs with 100 different seeds (initial factor
 424 profiles) were performed. The results of those analyses (Figure S4) show that a 3-factor PMF result is robust. A PMF
 425 analysis was performed on the consolidated time series of all coniferous fuels fit using just the N_r species, as shown
 426 in Figure S5. In this case Fpeak=0 was used and the Q/Qexpected showed an inflection for the 3-factor solution at a
 427 value of 5.3 The three factors successfully describe the majority of the N_r -emissions where the difference between the
 428 measured and calculated mass is on average 5.1% for coniferous fuels and 4.6% for chaparrals as indicated in Table
 429 4.

430 Several metrics of the PMF analysis quantify how the compounds or compound classes contribute to each
 431 factor. The ‘loadings’ of the three different factors, i.e. the contribution of compounds to each factor, for coniferous
 432 fuels are shown in Figure 9(a), and the distribution of a given compound or compound class amongst the three factors
 433 is shown in Figure 9(b) as normalized fraction. Normalized fraction is equal to the PMF-determined contribution of a
 434 compound to a factor, divided by the sum of the contribution of the compound to all three factors. The Comb-N factor
 435 contained NO, NO_2 , and HONO, the HT-N factor had mostly HCN, HNCO, nitriles, with contributions from NO_2 and
 436 nitro compounds, and the LT-N factor contained NH_3 , amines, amides and heterocyclics. Within the Comb-N factor
 437 there is some evidence that the relative amounts of HONO and NO_x depend on fuel moisture. For example, the ratio
 438 HONO/ NO_x for whole fires shows some correlation with needle moisture in coniferous fires that were canopy fuels
 439 (Foliage and small woody biomass), as shown in Figure S6. This may be due to flame processes that interconvert NO_x
 440 and HONO in the presence of water vapor of OH (see Figure 1).

441 Literature values from studies where flame temperature was measured are typically in the range of 1100 –
 442 1200 °C (Taylor et al., 2004; Wotton et al., 2012), so we would assume that would constitute the upper range of our
 443 Comb-N factor. The radical chemistry involving HCN, HNCO and NH_3 starts to shut down below about 800-900°,
 444 according to the modeling of Glarborg et al., (2018), so we set 800°C as a lower limit for the Comb-N factor. The HT-
 445 N factor species are known to be produced by the intense pyrolysis of fuel N_r compounds (Hansson et al., 2004; Liu
 446 et al., 2018; Ren et al., 2010), which for these compounds becomes important at temperatures around 500-600°C.
 447 Accordingly, we estimate the temperature range for the HT-N factor at 500 – 800°C. The remaining LT-N factor
 448 results from mild pyrolysis and pertains to fire conditions of roughly 500°C and below, and was dominated by NH_3 ,
 449 amines, amides and some of the more complex organics (Koss et al., 2018). The names and temperature ranges are

approximate and likely include processes that occur inside flames as part of the flame proper, as turbulent diffusive flames are highly variable in space and time.

3.6 The comparison of N-PMF factors to other fire parameters and VOC emission factors.

It is useful to explore the correlation of N-PMF factors with other fire indicators to determine relationships for parameterizing N_r emissions together with carbon and VOC emissions, in order to simplify how emissions might be parameterized in models. The Comb-N factor for coniferous fuels, which consisted of NO_x and HONO, would be expected to correlate with CO_2 but not as well with MCE since the latter includes an indicator of incomplete combustion. The timeseries of Comb-N along with CO_2 and with MCE for Fire 037 (ponderosa pine), are plotted in Figure 10. As expected they show an excellent correlation of Comb-N with CO_2 ($R^2=0.942$) since all the species are flaming compounds, but non-linear correlation of Comb-N with MCE ($R^2=0.363$) since the latter factors in a smoldering compound (CO), similar to the NO_x/N_r vs. MCE plot for Fire 047 in Figure 7. The excellent correlation of Comb-N with CO_2 is a broadly applicable result, the R^2 parameters for all the fires shown in Figure S5 had an average of 0.898, and ranged from 0.806 to 0.966. As a consequence, we can conclude that CO_2 would be the best tracer for Comb-N in many western U.S. ecosystems where conifers predominate, provided ambient CO_2 backgrounds can be properly accounted for as described by Yokelson et al., (2013a).

Our Comb-N factor did not correspond to the high temperature VOC factor (HT-VOC) found by Sekimoto et al., (2018) in their pyrolysis study because our broader study includes flaming combustion, which produces NO_x , and HONO, and almost none of the compounds classified as VOCs survive flaming conditions. However, the HT-N and HT-VOC factors are both linked to pyrolysis and were well correlated for many fires. An example of this is shown in Figure 11 for Fire 037, a sample that was broadly representative of ponderosa pine (i.e. canopy and litter). This result can be rationalized by the fact that while HT-VOC factors have large contributions from many more compounds than the N compounds measured here, they also have large contributions (>85%) from HCN, HNCO, and HONO, (in other words >85% of HCN, HNCO and HONO are found in the HT-VOC factor). Since the HT-N factors are also heavily weighted by HCN and HNCO, it is reassuring that both of these PMF analyses have independently identified these species as important contributors to the HT fire regime. The R^2 correlation coefficients between the HT-N and HT-VOC factors for the coniferous fires shown in Figure S5 averaged 0.866 and ranged from 0.419 to 0.959. As a consequence of this correlation, we can conclude that HCN is the best marker for the HT-N and HT-VOC factors in most western U.S. wildfires, since HCN is essentially inert on the timescales of fire plumes (Li et al., 2000). It should be noted that other nitriles, particularly acetonitrile, also show up in the HT-N factor, and acetonitrile has also been used as a tracer of biomass combustion. However, it has been shown that this acetonitrile signal can be obscured in urban or industrial areas by solvent usage, or can be quite small in woodstove emissions due to low N in the fuel (Coggon et al., 2016).

The correlations of LT-N and LT-VOC factors were not particularly high for most of the coniferous fires shown in Figure S5. The average R^2 was 0.427 with a range of between 0.072 and 0.827. The reasons for this lack of correlation are not clear, as NH_3 , amines and amides appear predominantly in both LT factors, and the absolute concentrations of NH_3 are usually quite high in these fires relative to VOCs (Sekimoto et al., 2018). However, the LT-

VOC factor includes many more compounds with a variety of functional groups not found in the LT-N factor, so it appears that the VOC and N compounds have sufficiently different pyrolysis chemistry that the LT factors do not show much correlation. We conclude that NH₃ (and particle NH₄⁺) will be the best marker for the LT-N factor in western U.S. coniferous wildfires, but the LT-VOC chemistry might not be captured reliably by this marker.

3.7 PMF analysis of chaparral fuels.

Chaparral is an important ecosystem of concern in wildfires that occur in central and southern California, and other areas of the southwestern U.S. The emissions from burning chaparral fuels (manzanita and chamise) collected at two sites in California were also analyzed as a group and yielded three separate factors in a fashion similar to the coniferous fuels (see Figure S7 for the PMF timeline). As with the coniferous fuels, there was essentially no change in the 3-factor solution with F_{peak}, so F_{peak} 0 was used, and the Q/Q_{exp} was 3.8. The chaparral factors had slightly different composition (Figure S8), the combustion factor was mostly NO, with small amounts of HNCO, HONO and NH₃, the high temperature factor was dominated by NO₂ and included HONO, HCN, and HNCO, and the low temperature factor was mostly NH₃ with a slight amount of NO contributing. The NVOC species were found in both the medium and low temperature factors.

There was less similarity between the Comb-N factor and CO₂ emissions for chaparral fuels compared to those found for coniferous fuels, with an average correlation coefficient (R²) of 0.689, with a range from 0.244 and 0.950. As a result, there may not be a simple conserved tracer for the combustion factor of these fuel types, however total odd nitrogen (NO_y) which is NO_x and all the compounds that are produced from NO_x in the troposphere, may be useful as it is a reasonably conserved tracer in the absence of wet or dry deposition of particles. Correlation coefficients between the HT-N and HT-VOC factors were on average R² = 0.551, with a range 0.047-0.911. The correlations between LT-N and LT-VOC factors were in the same range for chaparral fuels as for coniferous, average R² = 0.447, range 0.028-0.827.

There were some fuels that do not sustain flaming combustion well, specifically duff, Yak dung and Indonesian peat. These fires exhibited little or no NO emission commensurate with minimal flaming combustion. Instead the emissions were mostly the pyrolysis products NH₃, (0.22 – 0.53 N_r fraction), and HCN (up to 0.32 N_r fraction for peat). It was also apparent that these fires also had unaccounted for N_r, close to, or just over 0.30 (Table S1). The distribution of N_r compounds in the one peat fire that we measured (Fire 055) is in line with those reported for fires measured in situ which showed relatively high EFs for HCN and NH₃ (Stockwell et al., 2016b; Stockwell et al., 2015).

3.8 Application to real-world fires.

The application of our N_r emissions results to real-world fires will depend somewhat on the nature of the information available on a particular fire, or fire complex. As a good starting point, or in the absence of detailed N and C analyses of fuels, a N_r/C ratio of 0.37% appears to capture most of the fires studied in this work. The N_r could be apportioned according to the results summarized in Table 3. Adjustments to those fractions can be made either by scaling slightly by average MCE, with the knowledge that intermediate species (HT-N pyrolysis species) such as HCN and HNCO do not scale in the simple manner that NH₃ and NO_x do. If measurements of marker compounds are

available then CO₂, HCN, and the sum NH₃ + NH₄⁺ can be used for the combustion, high-temperature pyrolysis, and low-temperature pyrolysis factors respectively.

4 Conclusions

Seventy-five stack fire experiments were conducted during the FIREX FireLab experiments in Fall, 2016. A range of fuels characteristic of the western U.S. was burned under conditions and in mixtures meant to represent authentic wildfire conditions, as closely as is possible in the laboratory. Total reactive nitrogen (N_r = all N-containing compounds except N₂ and N₂O) was measured along with a suite of N-containing compounds in order to obtain a budget for N_r-emissions and to examine relationships between fuels, combustion conditions, and emissions chemistry.

Natural convection wildfires do not burn hot enough to produce NO_x from N₂ and O₂, so all N_r emissions come from the fuel N. Almost all of the fires representative of North American ecosystems had emissions that clustered around a N_r/C ratio of 0.37%, which can serve as a starting point for scaling emissions from these ecosystems. Comparing total N_r and total carbon emissions with the N/C ratios of both the original fuel and remaining ash allowed us to estimate that an average of 68% (±14%) of the fuel nitrogen ends up as N₂ and N₂O. This loss of nitrogen can be used to estimate how much fuel nitrogen ends up as N_r. Of the remaining N emitted as N_r, approximately 85% (±10%) was accounted for by individually measured gas-phase species, while the rest was most likely particle-bound NH₄⁺ and NO₃⁻, with a smaller contribution from low-volatility species or other species such as cyanogen (Lobert and Warnatz, 1993), that were not quantified by the instruments for individual measurements we used in this study. The speciation and modeling of N_r we present promotes accurate modeling of fire plume chemistry since the photochemistry of many fire plumes is NO_x-limited, and NH₃ is an important contributor to particle chemistry.

The individual N_r species composition normalized to Total N_r, to account for fuel N variability, correlated monotonically with flaming versus smoldering combustion as indicated by modified combustion efficiency (MCE) for some species (e.g. NH₃, NO_x). Other species, such as HCN and HNCO, peaked at intermediate MCE values. Positive matrix factorization (PMF) showed that all the measured N_r emissions from the main two categories of fuels, conifers and chaparral, grouped into three mixtures (factors), roughly attributed to temperature: combustion (NO_x, HONO), high temperature (HNCO, HCN, nitriles), and low temperature (NH₃, amines, amides). Chemical kinetic and pyrolysis considerations set the temperature ranges for these regimes at approximately 800-1200°C, 500-800°C and <500°C respectively.

This paper connects mechanistic aspects of N combustion chemistry to the budget of N_r emissions from biomass burning. The emission composition measurements detailed here give useful information concerning what the initial conditions will be in actual fire plumes. These results suggest that for coniferous fuels characteristic of the western U.S. CO₂ is the best marker for flaming combustion, HCN is the best marker for high temperature pyrolysis processes, and NH₃/NH₄⁺ is the best marker for low temperature pyrolysis processes. The HT-N and HT-VOC pyrolysis factors showed high degree of correlation especially for coniferous fuels, which can simplify how these different classes of emissions can be estimated. Results from less comprehensive field experiments can be combined with this emissions information to improve the representation of N_r-chemistry in the modeling frameworks needed to predict fire plume chemistry and impacts.

561

562 **Data availability**

563 The FIREX Firelab 2016 data are available at:

564 <https://esrl.noaa.gov/csd/groups/csd7/measurements/2016firex/FireLab/DataDownload/>. The descriptions of the
565 measurements can be found here:

566 <https://esrl.noaa.gov/csd/groups/csd7/measurements/2016firex/FireLab/dataidtable.html>. The complete ash analyses
567 are available on request.
568

569 **Author Contributions**

570 JMR, RY, CW and JdG designed the research. The measurements were conducted by JMR, CS, CW, RJY,
571 JdG, YL, VS, ARK, KS, MMC, BY, KJZ, SSB, CS, and SHD. All authors contributed to the discussion and
572 interpretation of the results and writing the paper.
573

574 **Competing interests**

575 Joost de Gouw worked as a consultant for Aerodyne Research during part of the preparation phase of this
576 paper.
577

578 **Disclaimer**

579 Any mention of brand names or manufacturers is for information purposes only and does not constitute an
580 endorsement.
581

582 **Acknowledgements**

583 A. Koss acknowledges funding from the NSF Graduate Fellowship Program. K. Sekimoto acknowledges
584 funding from the Postdoctoral Fellowships for Research Abroad from Japan Society for the Promotion of Science
585 (JSPS) and a Grant-in-Aid for Young Scientists (B) (15K16117) from the Ministry of Education, Culture, Sports,
586 Science and Technology of Japan. R. Yokelson and V. Selimovic were supported by NOAA-CPO grant
587 NA16OAR4310100. J. de Gouw was supported by the NSF AGS grant 1748266 under a subcontract to the University
588 of Montana during the analysis phase of this work. We thank the USFS Missoula Fire Sciences Laboratory for their
589 help in conducting these experiments, especially Shawn Urbanski and Thomas Dzomba. This work was also supported
590 by NOAA's Climate Research and Health of the Atmosphere Initiative^s.
591

592 **References**

- 593
594 Abatzoglou, J. T. and Williams, A. P.: Impact of anthropogenic climate change on wildfire across western
595 US forests, *Proc. Natl. Acad. Sci.*, 113, 11770-11775, 2016.
596
597 Akagi, S. K., Craven, J. S., Taylor, J. W., McMeeking, G. R., Yokelson, R. J., Burling, I. R., Urbanski, S.
598 P., Wold, C. E., Seinfeld, J. H., Coe, H., Alvarado, M. J., and Weise, D. R.: Evolution of trace gases and
599 particles emitted by a chaparral fire in California, *Atmos. Chem. Phys.*, 12, 1397-1421, 2012.
600
601 Akagi, S. K., Yokelson, R. J., Wiedinmyer, C., Alvarado, M. J., Reid, J. S., Karl, T., Crounse, J. D., and
602 Wennberg, P. O.: Emission factors for open and domestic biomass burning for use in atmospheric models,
603 *Atmos. Chem. Phys.*, 11, 4039-4072, 2011.
604
605 Alvarado, M. J., Logan, J. A., Mao, J., Apel, E., Riemer, D., Blake, D., Cohen, R. C., K.-E., M., Perring,
606 A. E., Browne, E. C., Wooldridge, P. J., Diskin, G. S., Sachse, G. W., Fuelberg, H., Sessions, W. R.,
607 Harrington, D. L., Huey, L. G., Liao, J., Case-Hanks, A., Jimenez, J. L., Cubison, M. J., Vay, S. A.,
608 Weinheimer, A. J., Knapp, D. J., Montzka, D. D., Flocke, F. M., Pollack, I. B., Wennberg, P. O., Kurten,
609 A., Crounse, J. D., St. Clair, J. M., Wisthaler, A., Mikoviny, T., Yantosca, R. M., Carouge, C. C., and Le

Sager, P.: Nitrogen oxides and PAN in plumes from boreal fires during ARCTAS-B and their impact on ozone: an integrated analysis of aircraft and satellite observations, *Atmos. Chem. Phys.*, 10, 9739-9760, 2010.

Andreae, M. O.: Emission of trace gases and aerosols from biomass burning – an updated assessment, *Atmos. Chem. Phys.*, 19, 8523-8546, 2019.

Andreae, M. O. and Merlet, P.: Emission of trace gases and aerosols from biomass burning, *Global Biogeochem. Cycles*, 15, 955-966, 2001.

Benedict, K. B., Prenni, A. J., Carrico, C. M., Sullivan, A. P., Schichtel, B. A., and Collett Jr., J. L.: Enhanced concentrations of reactive nitrogen species in wildfire smoke, *Atmos Environ.*, 148, 8-15, 2017.

Burling, I. R., Yokelson, R. J., Griffith, D. W. T., Johnson, T. J., Veres, P., Roberts, J. M., Warneke, C., Urbanski, S. P., Reardon, J., Weise, D. R., Hao, W. M., and de Gouw, J.: Laboratory measurements of trace gas emissions from biomass burning of fuel types from the southeastern and southwestern United States, *Atmos. Chem. Phys.*, 10, 11115-11130, 2010.

Christian, T. J., Kleiss, B., Yokelson, R. J., Holzinger, R., Crutzen, P. J., Hao, W. M., Shirai, T., and Blake, D. R.: Comprehensive laboratory measurements of biomass-burning emissions: 2, First intercomparison of open path FTIR, PTR-MS, GC-MS/FID/ECD, *J. Geophys. Res.*, 109, D02311, 2004.

Coggon, M., Veres, P. R., Yuan, B., Koss, A. R., Warneke, C., Gilman, J. B., Lerner, B., Peischl, J., Aikin, K., Stockwell, C. E., Hatch, L. E., Ryerson, T. B., Roberts, J. M., Yokelson, R. J., and de Gouw, J.: Emissions of nitrogen-containing organic compounds from the burning of herbaceous and arboraceous biomass: fuel composition dependence and the variability of commonly used nitrile tracers, *Geophys. Res. Lett.*, 43, 9903-9912, 2016.

Crutzen, P. J. and Andreae, M. O.: Biomass burning in the tropics: Impact on atmospheric chemistry and biogeochemical cycles, *Science*, 250, 1669-1678, 1990.

Gilman, J. B., Lerner, B. M., Kuster, W. C., Goldan, P. D., Warneke, C., Veres, P. R., Roberts, J. M., deGouw, J. A., Burling, I. R., and Yokelson, R. J.: Biomass burning emissions and potential air quality impacts of volatile organic compounds and other trace gases from temperate fuels common to the United States, *Atmos. Chem. Phys.*, 15, 13915-13938, 2015.

Glarborg, P., Miller, J. A., Ruscic, B., and Klippenstein, S. J.: Modeling nitrogen chemistry in combustion, *Prog. Energy Comb. Sci.*, 67, 31-68, 2018.

Griffith, D. W. T., Mankin, W. G., Coffey, M. T., Ward, R. E., and Riebau, A.: FTIR remote sensing of biomass burning emissions of CO₂, CO, CH₄, CH₂O, NO, NO₂, NH₃, and N₂O. In: *Global Biomass Burning: Atmospheric, Climatic, and Biospheric Implications*, Levine, J. S. (Ed.), The MIT Press, Cambridge, MA, 1991.

Hansson, K.-M., Samuelsson, J., Tullin, C., and Amand, L.-E.: Formation of HNCO, HCN, and NH₃ from the pyrolysis of bark and nitrogen-containing model compounds, *Combust. Flame*, 137, 265-277, 2004.

Hao, W. M., Scharffe, D. H., Lobert, J. M., and Crutzen, P. J.: Emissions of N₂O from the burning of biomass in an experimental system, *Geophys. Res. Lett.*, 18, 999-1002, 1991.

Hardy, J. E. and Knarr, J. J.: Technique for measuring the total concentration of gaseous fixed nitrogen species, *J. Air Pollut. Contr. Assoc.*, 32, 376-379, 1982.

Jayarathne, T., Stockwell, C. E., Bhawe, P. V., Praveen, P. S., Rathnayake, C. M., Islam, M. R., Panday, A. K., Adhikari, S., Maharjan, R., Goetz, J. D., DeCarlo, P. F., Saikawa, E., Yokelson, R. J., and Stone, E. A.: Nepal Ambient Monitoring and Source Testing Experiment (NAMaSTE): emissions of particulate matter from wood- and dung-fueled cooking fires, garbage and crop residue burning, brick kilns, and other sources, *Atmos. Chem. Phys.*, doi: 10.5194/acp-18-2259-2018, 2018. 2259-2286, 2018.

Jen, C. N., Hatch, L. E., Selimovic, V., Yokelson, R. J., Weber, R., Fernandez, A. E., Kreisberg, N. M., Barsanti, K. C., and Goldstein, A. H.: Speciated and total emission factors of particulate organics from burning western US wildland fuels and their dependence on combustion efficiency, *Atmos. Chem. Phys.*, 19, 1013-1026, 2019.

Kashihira, N., Makino, K., Kirita, K., and Watanabe, Y.: Chemiluminescent nitrogen detector-gas chromatography and its application to measurement of atmospheric ammonia and amines, *J. Chromatogr.*, 239, 617-624, 1982.

Koss, A. R., K., S., Gilman, J. B., Selimovic, V., Coggon, M. M., Zarzana, K. J., Yuan, B., Lerner, B. M., Brown, S. S., Jimenez, J. L., J., K., Roberts, J. M., Warneke, C., Yokelson, R. J., and de Gouw, J.: Non-methane organic gas emissions from biomass burning: identification, quantification, and emission factors from PTR-ToF during the FIREX 2016 laboratory experiment, *Atmos. Chem. Phys.*, 18, 3299-3319, 2018.

Kuhlbusch, T. A., Lobert, J. M., Crutzen, P. J., and Warneck, P.: Molecular nitrogen emissions from denitrification during biomass burning, *Nature*, 351, 135-137, 1991.

[Lee, B. H., Lopez-Hilfiker, F. D., Mohr, C., Kurten, T., Worsnop, D. R., and Thornton, J. A.: An Iodide-Adduct High-Resolution Time-of-Flight Chemical-Ionization Mass Spectrometer: Application to Atmospheric Inorganic and Organic Compounds, *Environ. Sci. Technol.*, 48, 6309-6317, 2014.](#)

Lee, D. C., Quigley, T. M., Norman, S., Christie, W., Fox, J., Rogers, K., and Hutchins, M.: National Cohesive Wildland Fire Management Strategy, U.S. Department of the Interior, Washington, D.C., 2014.

[Lerner, B. M., Gilman, J. B., Aikin, K. C., Atlas, E. L., Goldan, P. D., Graus, M., Hendershot, R., Isaacman-VanWertz, G. A., Koss, A. R., Kuster, W. C., Lueb, R. A., McLaughlin, R. J., Peischl, J., Sueper, D. T., Ryerson, T. B., Tokarek, T. W., Warneke, C., Yuan, B., and deGouw, J. A.: An improved, automated whole air sampler and gas chromatography mass spectrometry analysis system for volatile organic compounds in the atmosphere, *Atmos. Meas. Tech.*, 10, 291-313, 2017.](#)

Liu, X., Huey, L. G., Yokelson, R. J., Selimovic, V., I.J., S., Muller, M., Jimenez, J. L., Campuzano-Jost, P., Beyersdorf, A. J., Blake, D. R., Butterfield, Z., Choi, Y., Crounse, J. D., Day, D. A., Diskin, G. S., Dubey, M. K., Fortner, E., Hanisco, T. F., Hu, W., King, L. E., L., K., Meinardi, S., Mikoviny, T., Onasch, T. B., Palm, B. B., Peischl, J., Pollack, I. B., Ryerson, T. B., Sachse, G. W., Sedlacek, A. J., Shilling, J. E., Springston, S. R., St. Clair, J. M., Tanner, D. J., Teng, A. P., Wennberg, P. O., Wisthaler, A., and Wolfe, G. M.: Airborne measurements of western U.S. wildfire emissions: Comparison with prescribed burning and air quality implications, *J. Geophys. Res.*, 122, 6108-6129, 2017.

Liu, X., Luo, Z., Yu, C., Jin, B., and Tu, H.: Release mechanism of fuel-N into NO_x and N₂O precursors during pyrolysis of rice straw, *Energies*, 11, 520, 2018.

711 Liu, X., Zhang, Y., Huey, L. G., Yokelson, R. J., Wang, Y., Jimenez, J. L., Campuzano-Jost, P.,
 712 Beyersdorf, A. J., Blake, D. R., Choi, Y., St. Clair, J. M., Crounse, J. D., Day, D. A., Diskin, G. S., Fried,
 713 A., Hall, S. R., Hanisco, T. F., King, L. E., Meinardi, S., Mikoviny, T., Palm, B. B., J., P., A.E., P.,
 714 Pollack, I. B., Ryerson, T. B., Sachse, G. W., Schwarz, J. P., Simpson, I. J., Tanner, D. J., Thornhill, K.
 715 L., Ullman, K., Weber, R. J., Wennberg, P. O., Wisthaler, A., Wolfe, G. M., and Ziemba, L. D.:
 716 Agricultural fires in the southeastern U.S. during SEAC⁴RS: Emissions of trace gases and particles and
 717 evolution of ozone, reactive nitrogen, and organic aerosol, *J. Geophys. Res.*, 121, 7383-7414, 2016.
 718
 719 Lobert, J. M., Scharffe, D. H., Hao, W.-M., Kuhlbusch, T. A., Seuwen, R., Warneck, P., and Crutzen, P.
 720 J.: Experimental evaluation of biomass burning emissions: Nitrogen and carbon containing compounds.
 721 In: *Global Biomass Burning: Atmospheric, Climatic, and Biospheric Implications*, Levine, J. S. (Ed.), The
 722 MIT Press, Cambridge, MA, 1991.
 723
 724 Lobert, J. M., Scharffe, D. H., Hao, W. M., and Crutzen, P. J.: Importance of biomass burning in the
 725 atmospheric budgets of nitrogen-containing gases, *Nature*, 346, 552-554, 1990.
 726
 727 Lobert, J. M. and Wornatz, J.: Emissions from the combustion process in vegetation. In: *Fire in the*
 728 *Environment: The Ecological, Atmospheric and Climatic Importance of Vegetation Fires*, Crutzen, P. J.
 729 and Goldammer, J. G. (Eds.), John Wiley and Sons, New York, N.Y., 1993.
 730
 731 [Li, Q., Jacob, D. J., Bey, I., Yantosca, R. M., Zhao, Y., Kondo, Y., and Notholt, J.: Atmospheric](#)
 732 [hydrogen cyanide \(HCN\): Biomass burning sources, ocean sink?, *Geophys. Res. Lett.*, 27, 357-360, 2000.](#)
 733
 734 Lucassen, A., Zhang, K., Warkentin, J., Mashhammer, K., Glarborg, P., Marshall, P., and Kohse-
 735 Hoinghaus, K.: Fuel-nitrogen conversion in the combustion of small amines using dimethylamine and
 736 ethylamine as biomass-related model fuels, *Combust. Flame*, 159, 2254-2279, 2012.
 737
 738 Manfred, K. M., Washenfelder, R. A., Wagner, N. L., Adler, G., Erdesz, F., Womack, C. C., Lamb, K. D.,
 739 Schwarz, J. P., Franchin, A., Selimovic, V., Yokelson, R. J., and Murphy, D. M.: Investigating biomass
 740 burning aerosol morphology using a laser imaging nephelometer, *Atmos. Chem. Phys.*, 18, 1879-1894,
 741 2018.
 742
 743 Manion, J. A., Huie, R. E., Levin, R. D., Burgess Jr., D. R., Orkin, V. L., Tsang, W., McGivern, W. S.,
 744 Hudgens, J. W., Knyazev, V. D., Atkinson, D. B., Cahi, E., Tereza, A. M., Lin, C.-Y., Allison, T. C.,
 745 Mallard, W. G., Westley, F., Herron, J. T., Hampson, R. F., and Frizzell, D. H.: <http://kinetics.nist.gov/>,
 746 2015.
 747
 748 Marx, O., Brummer, C., Ammann, C., Wolff, V., and Freibauer, A.: TRANC – a novel fast-response
 749 converter to measure total reactive atmospheric nitrogen, *Atmos. Meas. Tech.*, 5, 1045-1057, 2012.
 750
 751 May, A. A., McMeeking, G. R., Lee, T., Taylor, J. W., Craven, J. S., Burling, I. R., Sullivan, A. P.,
 752 Akagi, S. K., Collett, J. L. J., Flynn, M., Coe, H., Urbanski, S. P., Seinfeld, J. H., Yokelson, R. J., and
 753 Kreidenweis, S. M.: Aerosol emissions from prescribed fires in the United States: A synthesis of
 754 laboratory and aircraft measurements, *J. Geophys. Res.*, 119, 2014.
 755
 756 McMeeking, G. R., Kreidenweis, S. M., Baker, S., Carrico, C. M., Chow, J. C., Collett Jr., J. L., Hao, W.
 757 M., Holden, A. S., Kirchstetter, T. W., Malm, W. C., Moosmuller, H., Sullivan, A. P., and Wold, C. E.:
 758 Emissions of trace gases and aerosols during the open combustion of biomass in the laboratory, *J.*
 759 *Geophys. Res.*, 114, doi:10.1029/2009JD011836, 2009.
 760

Field Code Changed

Min, K. E., Washenfelder, R. A., Dube, W. P., Langford, A. O., Edwards, P. M., Zarzana, K. J., Stutz, J., Lu, K., Rohrer, F., Zhang, Y., and Brown, S. S.: A broadband cavity enhanced absorption spectrometer for aircraft measurements of glyoxal, methylglyoxal, nitrous acid, nitrogen dioxide, and water vapor, *Atmos. Meas. Tech.*, 9, 423-440, 2016.

NOAA: <https://www.esrl.noaa.gov/csd/projects/firex/2018>.

Paatero, P. and Tapper, U.: Positive matrix factorization: A non-negative factor model with optimal utilization of error estimates of data values. , *Environmetrics*, 5, 111-126, 1994.

Prenni, A. J., Levin, E. J. T., Benedict, K. B., Sullivan, A. P., Schurman, M. I., Gebhart, K. A., Day, D. E., Carrico, C. M., Malm, W. C., Schichtel, B. A., Collett Jr., J. L., and Kreidenweis, S. M.: Gas-phase reactive nitrogen near Grand Teton National Park: Impacts of transport, anthropogenic emissions, and biomass burning, *Atmos Environ.*, 89, 749-756, 2014.

Ren, Q. Q., Zhao, C. S., Wu, X. X., Liang, C., Chen, X. P., Shen, J. Z., and Wang, Z.: Formation of NO_x precursors during wheat straw pyrolysis and gasification with O₂ and CO₂, *Fuel*, 89, 1064-1069, 2010.

Roberts, J. M., Langford, A. O., Goldan, P. D., and Fehsenfeld, F. C.: Ammonia measurements at Niwot Ridge, Colorado, and Point Arena, California, using the tungsten oxide denuder tube technique, *J. Atmos. Chem.*, 7, 137-152, 1988.

Roberts, J. M., Veres, P. R., Cochran, A. K., Warneke, C., Burling, I. R., Yokelson, R. J., Lerner, B. M., Gilman, J. B., Kuster, W. C., Fall, R., and de Gouw, J.: Isocyanic acid in the atmosphere and its possible link to smoke-related health effects, *PNAS*, 108, 8966-8971, 2011.

Saylor, R. D., Edgerton, E. S., Hartsell, B. E., Baumann, K., and Hansen, D. A.: Continuous gaseous and total ammonia measurements from the southeastern aerosol research and characterization (SEARCH) study, *Atmos. Environ.*, 44, 4994-5004, 2010.

Schwab, J. J., Li, Y., Bae, M.-S., Demerjian, K. L., Hou, J., Zhou, X., Jensen, B., and Pryor, S.: A laboratory intercomparison of real-time gaseous ammonia measurement methods, *Environ. Sci. Technol.*, 41, 8412-8419, 2007.

Sekimoto, K., Li, S.-M., Yuan, B., Koss, A. R., Coggon, M. M., Warneke, C., and de Gouw, J.: Calculation of the sensitivity of proton-transfer-reaction mass spectrometry (PTR-MS) for organic trace gases using molecular properties, *Int. J. Mass Spectrom.*, 421, 71-94, 2017.

Sekimoto, K., Koss, A. R., Gilman, J. B., Selimovic, V., Coggon, M. M., Zarzana, K. J., Yuan, B., Lerner, B. M., Brown, S. S., Warneke, C., Yokelson, R. J., Roberts, J. M., and de Gouw, J.: High- and low-temperature pyrolysis profiles describe primary emissions of volatile organic compounds from western US wildfire fuels, *Atmos. Chem. Phys.*, 18, 9263-9281, 2018.

Selimovic, V., Yokelson, R. J., Warneke, C., Roberts, J. M., deGouw, J. A., Reardon, J., and Griffith, D. W. T.: Aerosol optical properties and trace gas emissions by PAX and OP-FTIR for laboratory-simulated western US wildfires during FIREX, *Atmos. Chem. Phys.*, 18, 2929-2948, 2018.

Shaddix, C. R., Harrington, J. E., and Smyth, K. C.: Quantitative measurements of enhanced soot production in a flickering methane/air diffusion flame, *Combust. Flame*, 99, 723-732, 1994.

Stockwell, C. E., Christian, T. J., Goetz, J. D., Jayarathne, T., Bhawe, P. V., Praveen, P. S., Adhikari, S., Maharjan, R., DeCarlo, P. F., Stone, E. A., Saikawa, E., Blake, D. R., Simpson, I. J., Yokelson, R. J., and

Field Code Changed

Panday, A. K.: Nepal Ambient Monitoring and Source Testing Experiment (NAMASte): emissions of trace gases and light-absorbing carbon from wood and dung cooking fires, garbage and crop residue burning, brick kilns, and other sources, *Atmos. Chem. Phys.*, 16, 11043-11081, 2016a.

Stockwell, C. E., Jayarathne, T., Cochrane, M. A., Ryan, K. C., Putra, E. I., Saharjo, B. H., Nurhayati, A. D., Albar, I., Blake, D. R., Simpson, I. J., Stone, E. A., and Yokelson, R. J.: Field measurements of trace gases and aerosols emitted by peat fires in Central Kalimantan, Indonesia, during the 2015 El Niño, *Atmos. Chem. Phys.*, 16, 11711 - 11732, 2016b.

Stockwell, C. E., Kupc, A., Witkowski, B., Talukdar, R. K., Liu, Y., Selimovic, V., Zarzana, K. J., Sekimoto, K., Warneke, C., Washenfelder, R. A., Yokelson, R. J., Middlebrook, A. M., and Roberts, J. M.: Characterization of a catalyst-based conversion technique to measure total particle nitrogen and organic carbon and comparison to a particle mass measurement instrument, *Atmos. Meas. Tech.*, 11, 2749-2768, 2018.

Stockwell, C. E., Veres, P. R., Williams, J., and Yokelson, R. J.: Characterization of biomass burning smoke from cooking fires, peat, crop residue and other fuels with high resolution proton-transfer-reaction time-of-flight mass spectrometry, *Atmos. Chem. Phys.*, 15, 845-865, 2015.

Stockwell, C. E., Yokelson, R. J., Kreidenweis, S. M., Robinson, A. L., DeMott, P. J., Sullivan, R. C., Reardon, J., Ryan, K. C., Griffith, D. W. T., and Stevens, L.: Trace gas emissions from combustion of peat, crop residue, domestic biofuels, grasses, and other fuels: configuration and Fourier transform infrared (FTIR) component of the fourth Fire Lab at Missoula Experiment (FLAME-4), *Atmos. Chem. Phys.*, 14, 9727-9754, 2014.

Taylor, S. W., Wotton, B. M., Alexander, M. E., and Dalrymple, G. N.: Variation in wind and crown fire behaviour in a northern jack pine-black spruce forest, *Canadian J. Forest Res.*, 34, 1561-1576, 2004.

Ulbrich, I. M., Canagaratna, M. R., Zhang, Q., Worsnop, D. R., and Jimenez, J. L.: Interpretation of organic components from Positive Matrix Factorization of aerosol mass spectrometric data, *Atmos. Chem. Phys.*, 9, 2891-2918, 2009.

Veres, P. R., Roberts, J. M., Burling, I. R., Warneke, C., de Gouw, J., and Yokelson, R. J.: Measurements of gas-phase inorganic and organic acids from biomass fires by negative-ion proton-transfer chemical-ionization mass spectrometry (NI-PT-CIMS), *J. Geophys. Res.-Atmos.*, 115, D23302, 2010.

Warneke, C., Roberts, J. M., Veres, P., Gilman, J. B., Kuster, W. C., Burling, I. R., Yokelson, R. J., and de Gouw, J. A.: VOC identification and inter-comparison from laboratory biomass burning using PTR-MS and PIT-MS, *Int. J. Mass Spectrom.*, 303, 6-14, 2011.

Westerling, A. L., Hidalgo, H. G., Cayan, D. R., and Swetnam, T. W.: Warming and Earlier Spring Increase Western U.S. Forest Wildfire Activity, *Science*, 313, 940-943, 2006.

Williams, E. J., Baumann, K., Roberts, J. M., Bertman, S. B., Norton, R. B., Fehsenfeld, F. C., Springston, S. R., Nunnermacker, L. J., Newman, L., Olszyna, K., Meagher, J., Hartsell, B., Edgerton, E., Pearson, J. R., and Rodgers, M. O.: Intercomparison of ground-based NO_y measurement techniques, *J. Geophys. Res.-Atmospheres*, 103, 22261-22280, doi: 10.1029/22298JD00074, 1998.

Wotton, B. M., Gould, J. S., McCaw, W. L., Cheney, N. P., and Taylor, S. W.: Flame temperature and residence time of fires in dry eucalypt forest, *Int. J. Wildland Fire*, 21, 270-281, 2012.

863 Yokelson, R. J., Andreae, M. O., and Akagi, S. K.: Pitfalls with the use of enhancement ratios or
 864 normalized excess mixing ratios measured in plumes to characterize pollution sources and aging, *Atmos.*
 865 *Meas. Tech.*, 6, 2155-2158, 2013a.
 866
 867 Yokelson, R. J., Burling, I. R., Gilman, J. B., Warneke, C., Stockwell, C. E., de Gouw, J. A., Akagi, S. K.,
 868 Urbanski, S. P., Veres, P., Roberts, J. M., Kuster, W. C., Reardon, J., Griffith, D. W. T., Johnson, T. J.,
 869 Hosseini, S., Miller, J. W., Cocker III, D. R., Jung, H., and Weise, D. R.: Coupling field and laboratory
 870 measurements to estimate the emission factors of identified and unidentified trace gases for prescribed
 871 fires, *Atmos. Chem. Phys.*, 13, 89-116, 2013b.
 872
 873 Yokelson, R. J., Crounse, J. D., DeCarlo, P. F., Karl, T., Urbanski, S., Atlas, E., Campos, T., Shinozuka,
 874 Y., Kapustin, V., Clarke, A. D., Weinheimer, A. J., Knapp, D. J., Montzka, D. D., Holloway, J.,
 875 Weibring, P., Flocke, F. M., Zheng, W., Toohey, D., Wennberg, P. O., Wiedinmyer, C., Mauldin, L.,
 876 Fried, A., Richter, D., Walega, J., Jimenez, J. L., Adachi, K., Buseck, P. R., Hall, S. R., and Shetter, R. E.:
 877 Emissions from biomass burning in the Yucatan, *Atmos. Chem. Phys.*, 9, 5785-5812, 2009.
 878
 879 Zarzana, K. J., Selimovic, V., Koss, A. R., Sekimoto, K., Coggon, M. M., Yuan, B., Dube, W. P.,
 880 Yokelson, R. J., Warneke, C., de Gouw, J. A., Roberts, J. M., and Brown, S. S.: Primary emissions of
 881 glyoxal and methylglyoxal from laboratory measurements of open biomass burning, *Atmos. Chem. Phys.*,
 882 18, 15451-15470, 2018.
 883
 884

885
886
887

Table 1. Nitrogen compounds observed in the FIREX FireLab 2016 Study.

Compound/Class	Importance	Measurement Method	<u>Method</u> Reference
Total Reactive N	Total available for atmospheric reactions	Catalytic Conversion NO/O ₃ chemiluminescence	Stockwell et al., 2018
Nitric Oxide	Major “flaming stage” product, oxidant production	NO/O ₃ chemiluminescence OP-FTIR (Open Path Fourier Transform Infrared)	Williams et al., 1998 Selimovic et al., 2018
Nitrogen Dioxide	Atmospheric oxidant production	OP-FTIR, ACES (Airborne Cavity-Enhanced Spectrometer)	Stockwell et al., 2014, Min et al., 2016, Zarzana, et al., 2018
Nitrous Acid	HO _x radical source	OP-FTIR, ACES	Stockwell et al., 2014, Min et al., 2016, Zarzana et al., 2018
Nitric Acid ¹	Particle precursor	OP-FTIR	Yokelson et al 2009, McMeeking et al 2009
Hydrogen Cyanide	Flame chemistry, Atmospheric tracer, Toxicity	OP-FTIR, PTR-ToF-MS (Proton Transfer Reaction Time of Flight Mass Spectrometer)	Selimovic, et al., 2018 Koss, et al., 2018
Isocyanic Acid	Flame chemistry, Toxicity, Health effects	PTR-ToF-MS	Koss, et al., 2018
Ammonia	Major “smoldering stage” product, Main atmospheric base, Particle formation	OP-FTIR	Selimovic, et al., 2018
NVOCs: Amides ² Amines ³ Heterocyclics ⁴ Nitriles ⁵ Nitro compds ⁶	Brown carbon, Toxicity, Tracers	PTR-ToF-MS, GC/MS (Gas Chromatography Mass Spectrometry), I ⁻ CIMS (Iodide ion Chemical Ionization Mass Spectrometer).	Koss, et al., 2018 Gilman et al., 2015 Lerner et al., 2017 Lee et al., 2014

888
889
890
891
892
893
894
895
896
897
898

- 1). The OP-FTIR has a 10ppbv detection for gas phase HNO₃, but HNO₃ was not observed above detection limit.
- 2). Ethylamine, methanimine, propeneamine, sulfinylmethanamine, trimethylamine, buteneamines
- 3). Formamide, acetamide, methylmaleimide
- 4). C₂-pyrroles, dihydropyridine, ethynylpyrrole, methylpyridine, methylpyrrole, pyridinealdehyde, 4-pyrindinol, vinylpyridine
- 5). Acetonitrile, acrylonitrile, benzonitrile, butanenitrile, butynenitrile, benzoacetonitrile, C₇acrylonitrile, C₈-nitriles, heptylnitrile, furancarbonitrile, methylbenzoacetonitrile, pentyl nitriles, propanenitrile, propynenitrile, butenenitrile, methylisocyanate.
- 6). Butenenitrates, nitrobenzene, nitroethane, nitroethene, nitrofuran, nitromethane, nitropropanes, nitrotoluene.

899 **Table 2. Compounds and compound classes used in the PMF analyses and their**
900 **corresponding errors.**

Compound or Class	unit	Estimated error
NH ₃	ppbv	5% + 2 ppbv
NO	ppbv	10% + 1 ppbv
NO ₂	ppbv	10% + 0.2 ppbv
HONO	ppbv	20% + 1 ppbv
HCN	ppbv	15% + 0.2 ppbv
HNCO	ppbv	15% + 0.2 ppbv
Nitriles	ppbv	20% + 0.2 ppbv
Amines	ppbv	20% + 0.2 ppbv
Amides	ppbv	20% + 0.2 ppbv
Nitro-compounds	ppbv	20% + 0.2 ppbv
Heterocyclics	ppbv	20% + 0.2 ppbv

903
904
905
906 **Table 3. Summary of X_i/N_r Measurements for all Stack Burns¹**

Quantity	Average ±(std dev) %
NO/N _r	34.5 (16.6)
NO ₂ /N _r	9.4 (6.2)
HNCO/N _r	6.0 (2.9)
HONO/N _r	4.5 (2.2)
HCN/N _r	4.3 (2.3)
NH ₃ /N _r	19.3 (6.7)
NVOC/N _r	4.3 (2.8)
(N _r -sumN)/N _r	15.2 (9.8)

908 1). Not every measurement was available for every fire, consequently the values do not add up to
909 exactly 100%.

910

911 **Table 4. Residuals of the PMF analyses by fuel, as percent of total signal**
912

Fuel	Total Number	Component	Fire Number	Residual (%), avg (stdev)
Ponderosa Pine	9	Realistic (mix)	Fire 37,59,72	3.8 (± 1.4)
		Canopy (pure)	Fire 19 ^a ,39	
		Litter (pure)	Fire 38	
Lodgepole Pine	5	Realistic	Fire 07 ^a ,58,63	5.1 (±3.1)
		Canopy	Fire 40	
		Litter	Fire 41	
Douglas Fir	4	Realistic	Fire 14 ^a ,57	6.8 (±3.1)
		Canopy	Fire 18	
		Litter	Fire 43 ^a	
SubAlpine Fir	5	Realistic	Fire 47,67	6.6 (±2.3)
		Canopy	Fire 15,23	
		Litter	Fire 51 ^a	
Engelmann Spruce	2	Realistic	Fire 08 ^a	3.1 (±1.9)
		Canopy	Fire 25	
Chamise (San Dimas, CA)	2	Canopy	Fire 24,29	4.4 (±2.7)
Chamise (North Mountain, CA.)	2	Canopy	Fire 27,32	4.2 (±1.0)
Manzanita San Dimas, CA)	2	Canopy	Fire 30,33	4.8 (±2.1)
Manzanita (North Mountain, CA.))	2	Canopy	Fire 28	5.1

a-Excluded from Batch 2

913
914
915

916
917

918
919
920
921
922
923
924
925
926
927

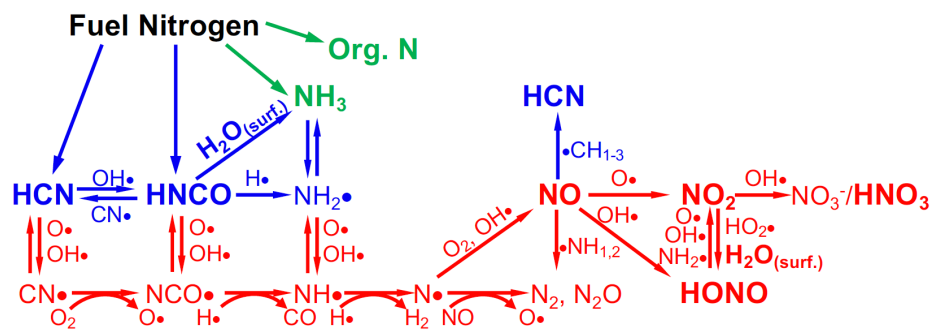
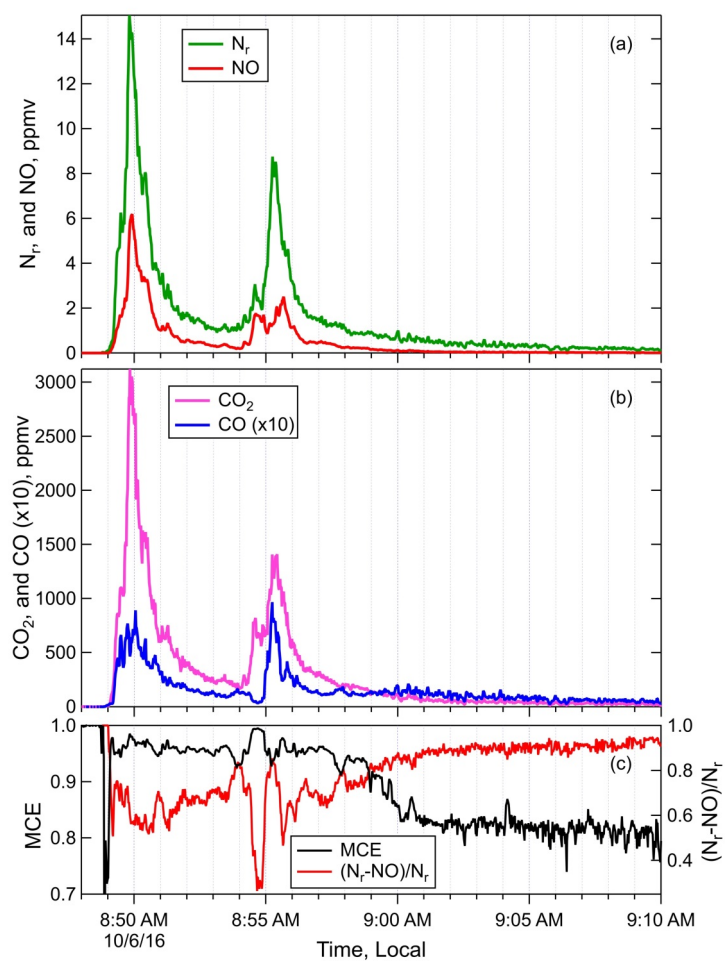


Figure 1. Schematic of the combustion chemistry of the small molecules that are emitted from BB and represent sources and sinks of reactive nitrogen (N_r), adapted from (Glarborg et al., 2018; Lobert and Warnatz, 1993; Lucassen et al., 2012; Manion et al., 2015). $H_2O_{(surf.)}$ denotes the combination of H_2O and a surface to facilitate the reaction. Red color indicates the highest temperature (combustion) processes, blue indicates intermediate temperature processes and green indicates the lowest temperature processes. The species that are measured in this work are shown in bold and slightly larger text.

928



929

930

931 **Figure 2. Timelines of the N_r , NO (panel a), ΔCO_2 , ΔCO (panel b), MCE and $(N_r-NO)/N_r$**
 932 **(panel c) measured during Fire 004, a ponderosa pine realistic mix sample. Note that ΔCO is**
 933 **plotted at x10 the measured abundance for clarity.**

934

935

936

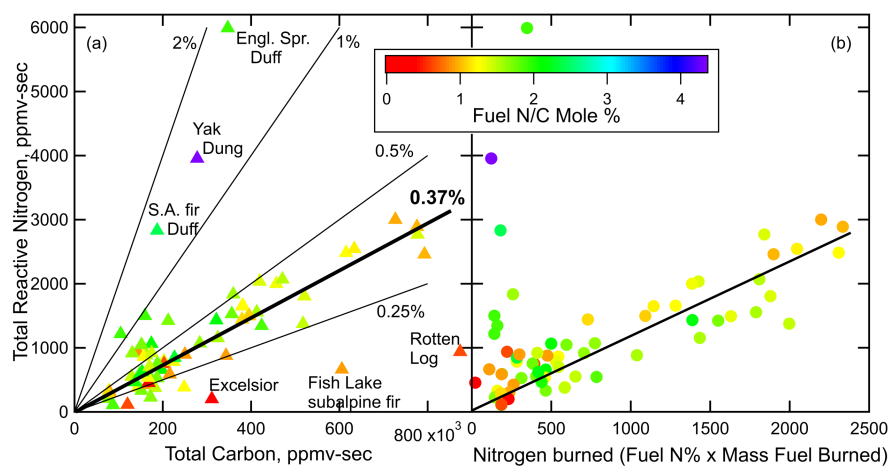
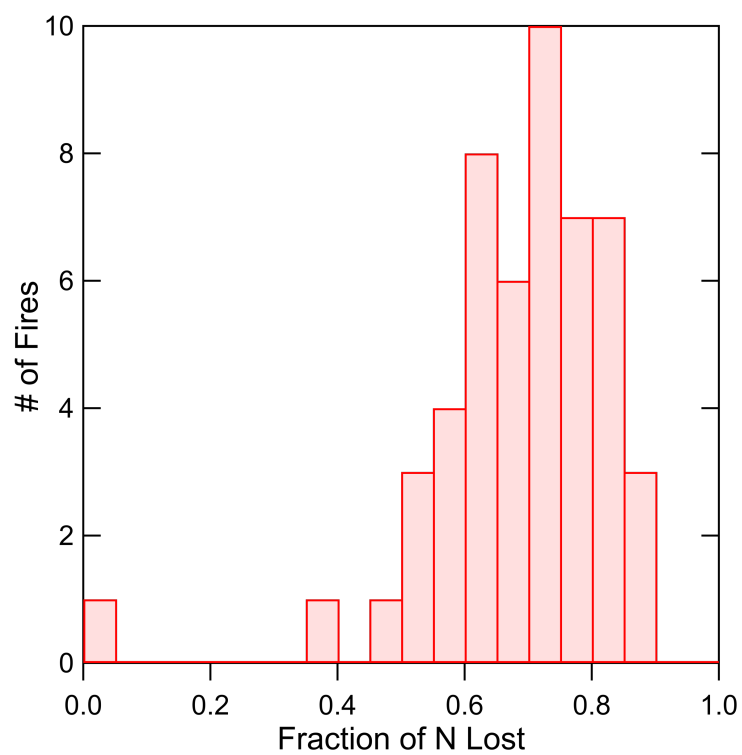


Figure 3. Integrated N_r versus integrated Total Carbon (panel a), and versus nitrogen burned based on fuel nitrogen content and mass of fuel burned (panel b). The points are colored by fuel nitrogen to carbon ratio. Note that the x and y scales on panel (a) are different by more than a factor of 100.

945
946



947
948
949
950

Figure 4. The histogram of the fraction of N loss to N_2 and N_2O estimated from the mass balance analysis described in the Supplemental Materials (52 burns).

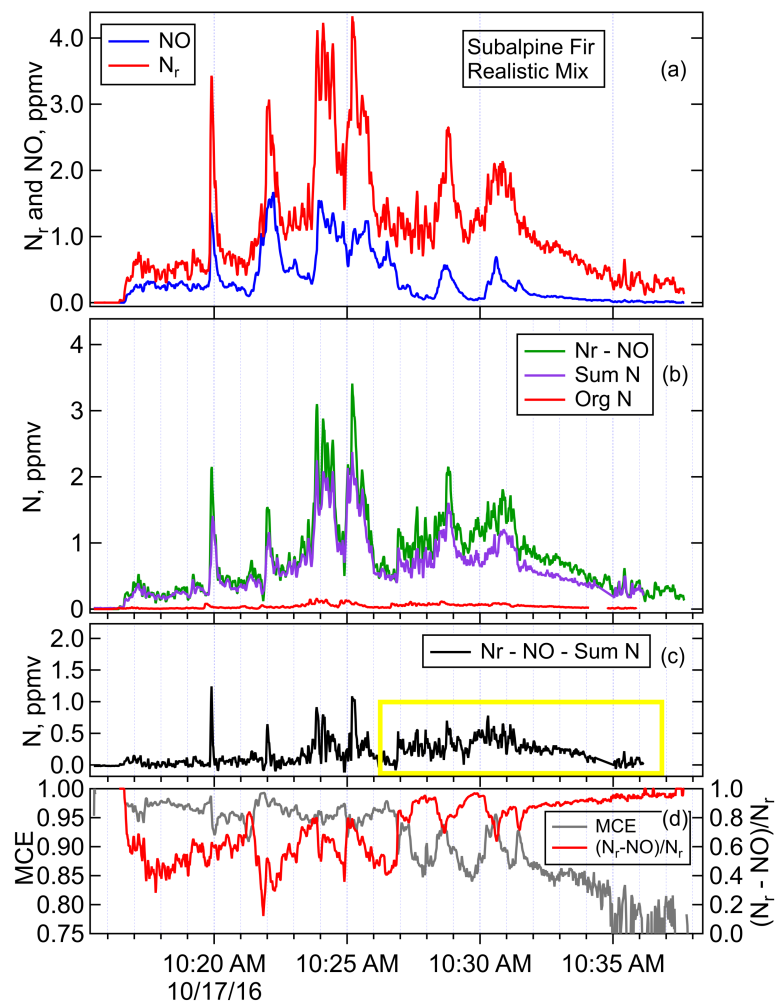


Figure 5. Timelines of N_r and NO (panel a), $N_r - NO$, the sum of all measures N species except for NO (panel b), residual of N_r minus all measured N species ($N_r - NO - \text{Sum N}$, panel c), and MCE and $(N_r - NO)/N_r$ (panel d) for Fire047, subalpine fir realistic mix. **The yellow box highlights the area of higher residual N_r that corresponds to more smoldering emissions.**

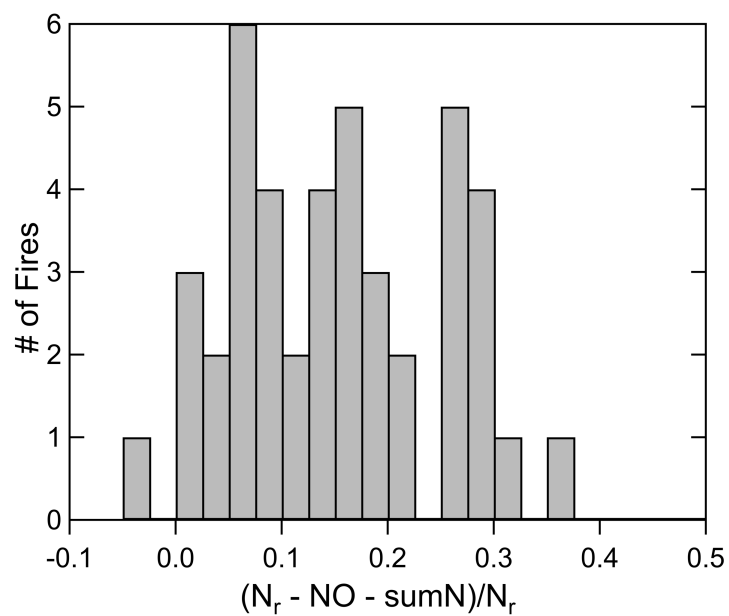
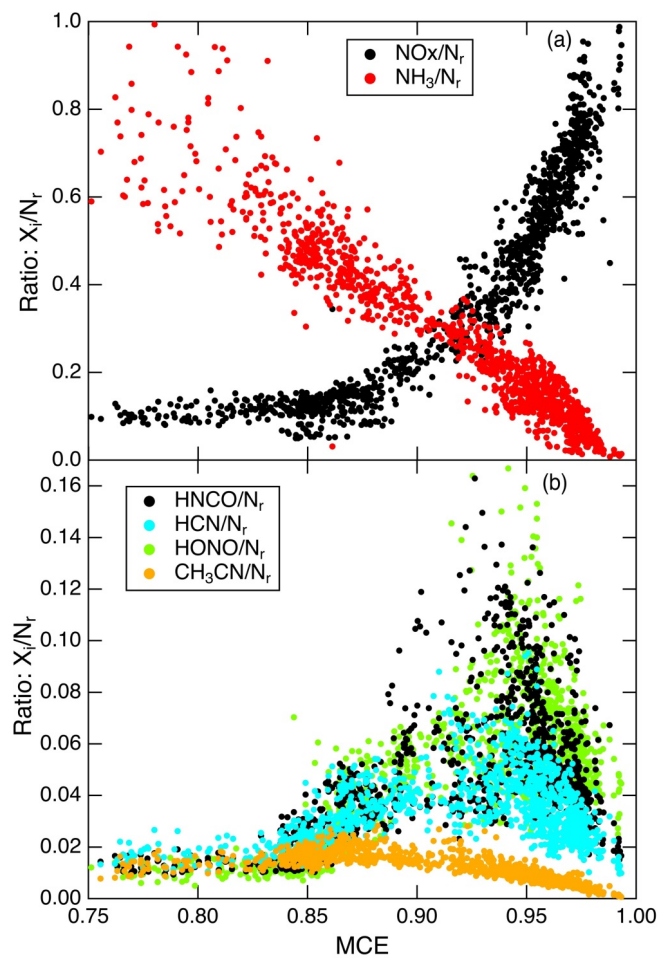


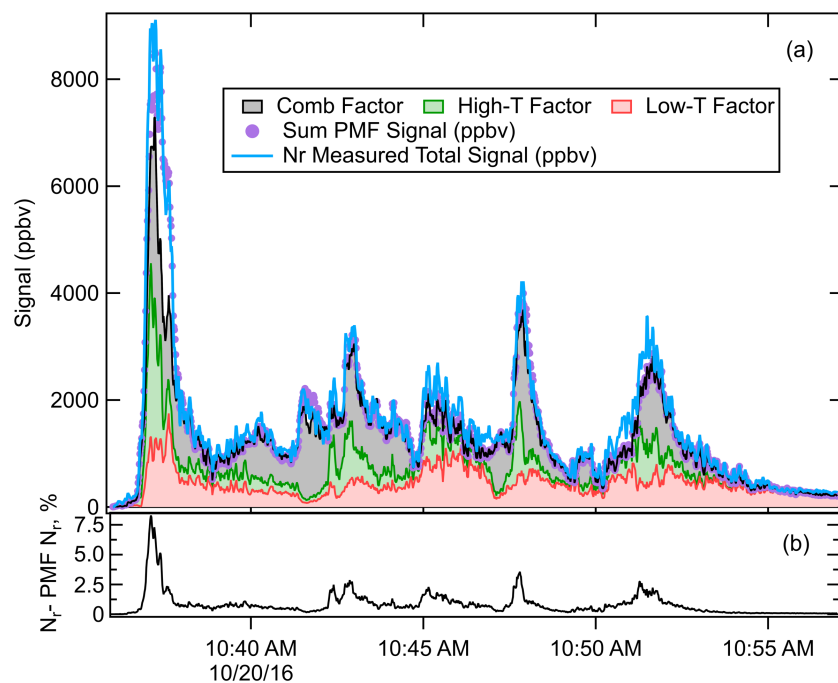
Figure 6. A histogram of the residual N for all the stack fires during the 2016 FireLab study for which there are FTIR, ACES and PTR-ToF measurements (n=43). The median is 0.143, and the mean (\pm std dev) was 0.15 (\pm 0.10).

969
970
971

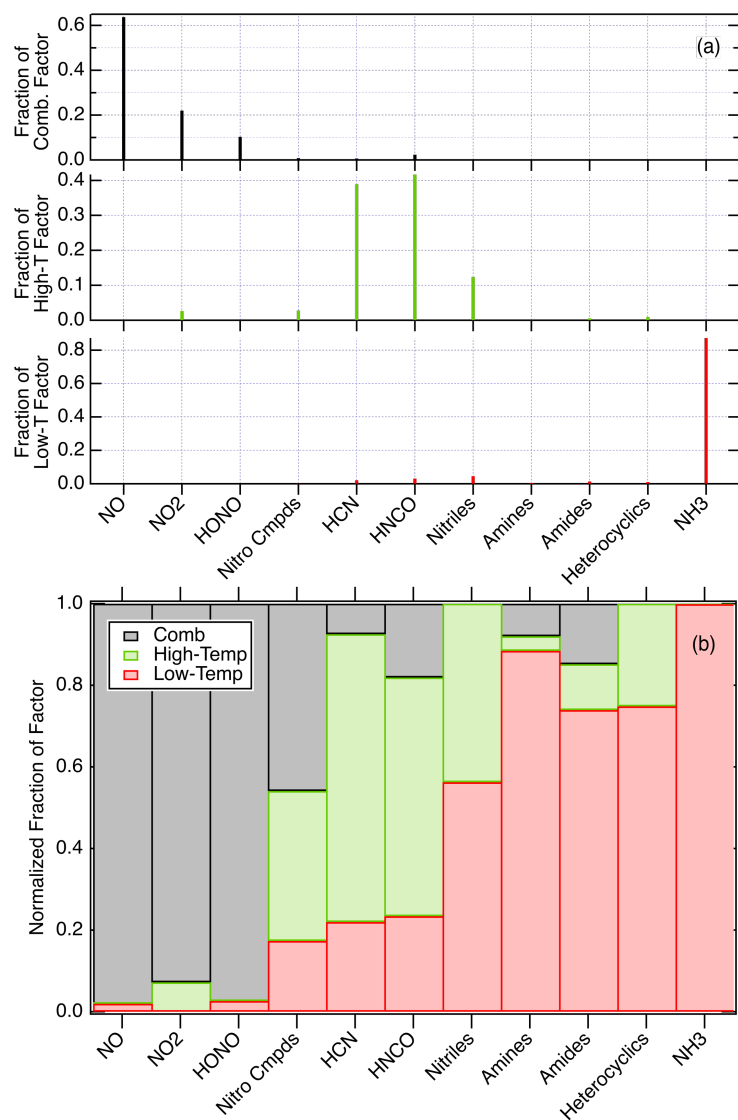


972
973
974
975
976
977

Figure 7. The relationships between NO_x/N_r and NH_3/N_r vs MCE (panel a), and the $HNCO/N_r$, HCN/N_r , $HONO/N_r$, and CH_3CN/N_r vs MCE (panel b) for Fire 047.



979
 980 **Figure 8.** Pane (a), the measured N_r signal for Fire 063 (lodgepole pine) (blue line), the sum
 981 of the signal reconstructed by the PMF (purple points) and the three PMF factors:
 982 combustion (grey), high temperature (green) and low temperature (red), plotted in a stacked
 983 fashion (i.e. added on top of one another). Panel (b) the “residual” of the PMF fit consisting
 984 of the measured N_r signal minus the N_r signal reconstructed by the PMF, as a percentage of
 985 the N_r signal.



986
987 **Figure 2.** The contributions of nitrogen species to the factors that simulate the emissions from
988 coniferous fuels shown in Figure S2 (panel a), and the fraction of each compound or class
989 found in each factor (panel b).

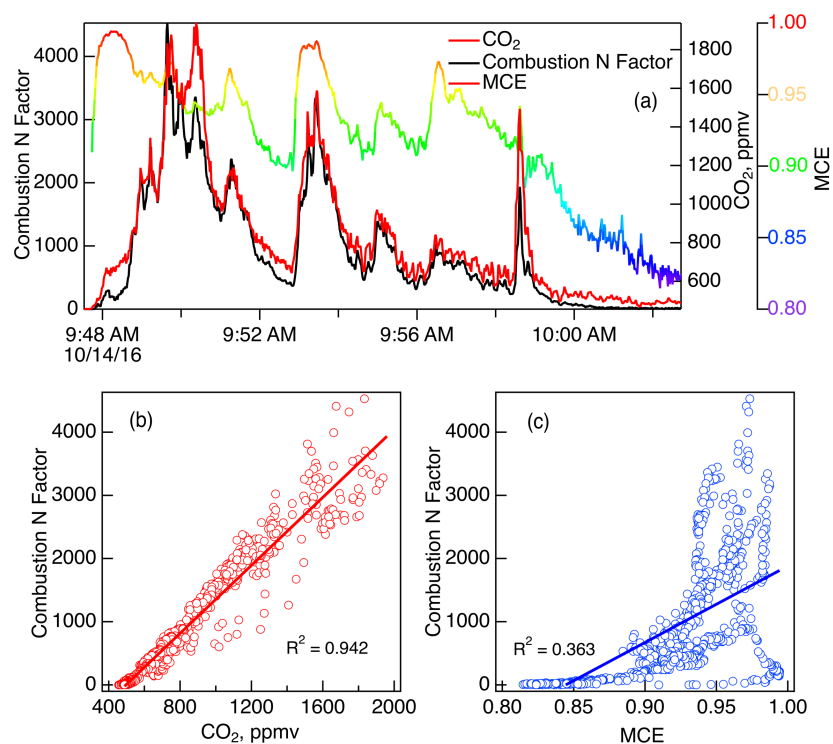


Figure 10. Comparisons of the N-PMF combustion factor (Comb-N) with CO₂ and MCE (Panel **a**) for Fire 037 (ponderosa pine). Panel **(b)** shows the scatter plot of the Comb-N factor versus CO₂ and panel **(c)** shows the scatter plot of Comb-N factor versus MCE.

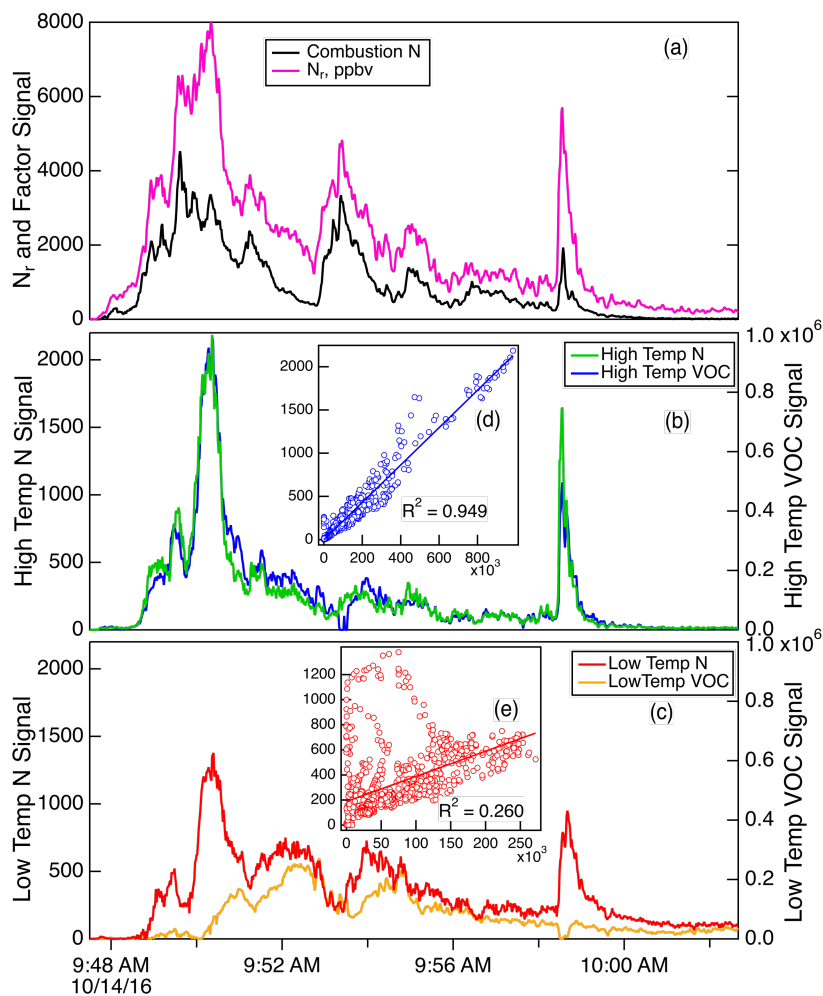


Figure 11. Details of the PMF factors for Fire 037 (ponderosa pine). Panel (a) shows the total N_r signal (magenta) and the Comb-N factor (black), panel (b) shows the HT-N factor (green) and HT-VOC factor (blue), and panel (c) shows the LT-N factor (red) and LT-VOC factor (orange). The insets (panel d) show the correlation of the two HT factors and the correlation between the two LT factors.